THE DESIGN AND CONSTRUCTION OF AN ACOUSTIC INSTRUMENT TO INVESTIGATE VIBRATIONAL RELAXATION TIMES IN OXYGEN AT HIGH TEMPERATURES

By

DENVER LEE PRINCE

Bachelor of Science
Henderson State Teachers College
Arkadelphia, Arkansas
1954

Master of Science-Education
University of Utah
Salt Lake City, Utah
1958

Submitted to the Faculty of the Graduate School of
the Oklahoma State University
in partial fulfillment of the requirements
for the degree of
DOCTOR OF EDUCATION
August, 1965

THE DESIGN AND CONSTRUCTION OF AN ACOUSTIC INSTRUMENT TO INVESTIGATE VIBRATIONAL RELAXATION TIMES IN OXYGEN AT HIGH TEMPERATURES

Thesis Approved:

Thomas G. Winter
Thesis Adviser

Helen M. Jones

Robert W. Scofield

H. E. Harrington

W. Ware Marsden

J. M. Boggs
Dean of the Graduate School

PREFACE

Vibrational relaxation time studies with oxygen have been undertaken by several individuals, but very little work has been done in the $500^{o}K$ to $1300^{o}K$ temperature range. Acoustic techniques have not been easy to apply to this temperature range, and shock tube work is useful only at higher temperatures.

Before acoustic measurements in the $500^{o}K$ to $1300^{o}K$ range can be made, an instrument to operate at these temperatures in an oxygen atmosphere must be designed and constructed. The purpose of this paper is to describe the design and construction of such a device, an acoustic instrument with which to measure the velocity and absorption of sound as functions of frequency.

Indebtedness is acknowledged to Dr. Thomas G. Winter for his guidance; Dr. H. E. Harrington for use of the Physics Department facilities; and the U.S. Army Research Office, Durham, North Carolina, for financial assistance.

TABLE OF CONTENTS

LIST OF TABLES

LIST OF FIGURES

CHAPTER I

INTRODUCTION

As the pressure maximum of a sound wave propagates through a gas there is an immediate increase in the translational energy of the gas, but there is some delay in raising the internal energy of the molecules (that is, their rotation and vibration). These time lags depend on the efficiency of molecular collision processes and are of importance for the understanding of chemical reactions. Practically, the thrust of a rocket motor or other type of high-intensity combustion device will depend on the state of the combustion products, and a knowledge of relaxation times may affect the optimum nozzle design.

In considering the mechanism by which energy enters the gas as internal energy, a good assumption is that a sudden compression of the gas should at first change the translational energy alone, but that, as a result of intermolecular collisions, the translational energy would be gradually converted into internal energy until a state of equilibrium was reached. It takes, on the average, a definite time for the gas to obtain this equilibrium state. Equilibrium is approached exponentially and the time constant of the process is defined as the molecular relaxation time.[1]

Relaxation effects can be measured acoustically. The speed of an

---

[1] J. L. Hunter, Acoustics (Prentice-Hall, Inc., N. J., 1957) pp. 348-349.

ordinary sound wave depends on the ratio of specific heats at constant pressure and constant volume, γ. At sufficiently low sound frequency the normal values for the specific heats will apply, but at high frequency there will not be time for the internal energy (particularly the vibrational energy) of the molecules to change, and so the specific heat will effectively be reduced thus making γ larger and the speed of sound will be higher. From measurement of the sound frequency at which this velocity change occurs, the relaxation time can be calculated. Alternatively, it is found that in the neighborhood of this critical frequency there is some absorption of the sound energy in the gas due to a partial flow of energy into vibration and then only a partial return to the wave during the final expansion; this frequency at which absorption occurs may therefore be measured instead. These acoustic methods have been used for measuring vibrational relaxation times and some rotational relaxation times, but have not been successfully used at temperatures above about $1000^{\circ}C$ and not this high with oxygen. The shock tube method has been used for measuring relaxation times at the high temperatures.[2]

Many experimental and theoretical investigations of thermal relaxation have been made[3] since the original suggestion by Herzfeld and Rice[4] that observed velocity dispersion and anomalous absorption in polyatomic gases are due to the slow rate of energy exchange between translational

---

[2] A. G. Gaydon and I. R. Hurle, The Shock Tube in High Temperature Chemical Physics (Reinhold Publishing Corp., New York, 1963), Chapter IX.

[3] K. F. Herzfeld and T. A. Litovitz, Absorption and Dispersion of Ultrasonic Waves (Academic Press Inc., New York, 1959).

[4] _____, and F. O. Rice, Phys. Rev. 31, 691 (1928).

and vibrational motion.

At room temperature the diatomic gas which has been examined most carefully is oxygen. The earliest measurements in oxygen appear to be those of Oberst[5] who found a relaxation time of 0.94 msec. Knötzel and Knötzel[6] measured sound velocity and absorption in oxygen-water and oxygen-ammonia mixtures, and, by extrapolating to zero impurity content, estimated the vibrational relaxation time of oxygen to be 3.1 msec. at one atmosphere; Henderson[7] reported that the results of measurements of absorption in oxygen at high pressures agreed with this. Smith and Wintle[8] measured velocity and absorption in oxygen at frequencies between 200 cps and 1300 cps and concluded that the vibrational relaxation time was 0.04 msec. Sound absorption measurements in oxygen-helium, oxygen-hydrogen and oxygen-deuterium mixtures were made by Parker[9] and by extrapolation of the oxygen-hydrogen results to zero impurity, he found a value of 18 ± 10 msec. for the relaxation time of oxygen. Smith and Tempest[10] found a relaxation time for oxygen of 3.1 msec.; but, while using the same apparatus with a better gas drying technique, Holmes, Smith and Tempest[11] found the relaxation time of oxygen at one atmosphere

---

[5] H. Oberst, Akust. Z. 2, 76 (1937).

[6] H. Knötzel and L. Knötzel, Ann. Phys. 2, 393 (1948).

[7] M. C. Henderson, J. Acoust. Soc. Am. 32, 1511 (1960).

[8] D. H. Smith and H. J. Wintle, J. Fluid Mech. 9, 29 (1960).

[9] J. G. Parker, J. Chem. Phys. 34, 1763 (1961).

[10] F. A. Smith and W. Tempest, J. Acoust. Soc. Am. 33, 1626 (1961).

[11] R. Holmes, F. A. Smith and W. Tempest, Proc. Phys. Soc. 81, 311 (1963).

pressure to be 15.9 ± 2.4 msec. which agreed well with Parker's results. Clark and Henderson[12] working with dry and moist oxygen, found the vibrational relaxation time for oxygen to be 17.7 msec. thus agreeing with Parker's results also. Shields and Lee[13] using an acoustic method determined the vibrational relaxation time of oxygen to be 1.71 msec. at 208.7°C and 1.01 msec. at 301.3°C which are considerably longer than would be expected by interpolation from previous data at higher and lower temperatures. Schnaus[14], using Henderson's[15] equipment with CH_4 and CD_4 mixtures has found the relaxation time for oxygen to be 15 msec. at 23°C.

Blackman[16] has used a shock tube method to measure relaxation times in oxygen at a series of temperatures above 772°K, but it is not possible to compare these with the work at around 300°K; thus, there is a need for work at the intermediate temperatures.

Figure 1, according to Shields and Lee[17], is a summary of previous work with the problem of vibrational collision number in pure oxygen. The vibrational collision number, Z, is the number of collisions needed to produce a 1/e approach to vibrational equilibrium and is determined from the relaxation time.

---

[12] A. V. Clark and M. C. Henderson, J. Acoust. Soc. Am. 35, 1909 (1963).

[13] F. D. Shields and Kun Pal Lee, J. Acoust. Soc. Am. 35, 251 (1963).

[14] U. E. Schnaus, J. Acoust. Soc. Am. 37, 1, (1965).

[15] M. C. Henderson and G. J. Donnelly, J. Acoust. Soc. Am. 34, 779 (1962).

[16] V. H. Blackman, J. Fluid Mech. 1, 61 (1956).

[17] F. D. Shields and Kun Pal Lee, J. Acoust. Soc. Am. 35, 251 (1963).

In Figure 1, log Z is plotted against $T^{-1/3}$. Both theory[18] and experiment[19] with other gases lead to the conclusion that an approximate linear relationship exists between these quantities.

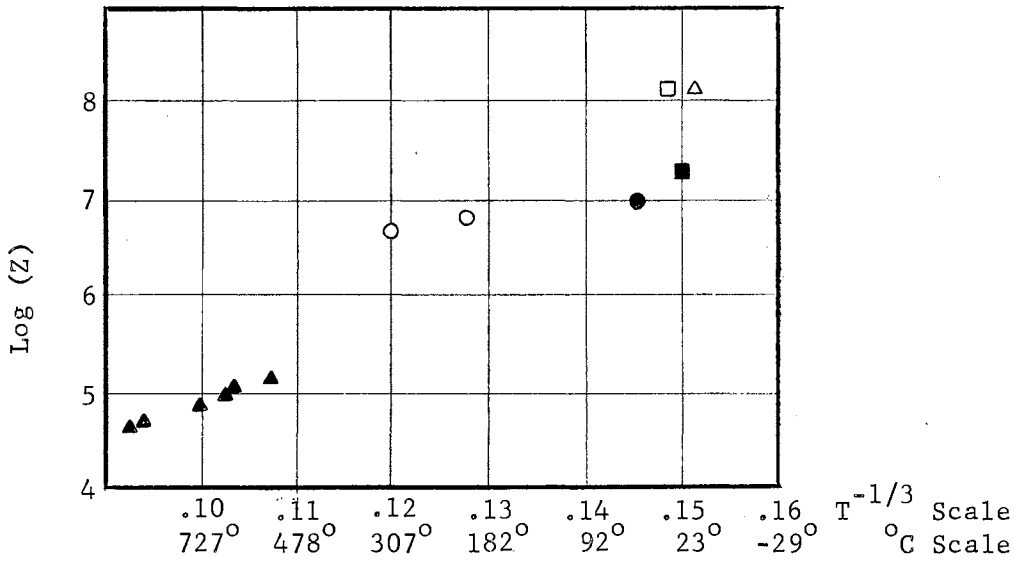

Figure 1. The temperature dependence of the vibrational collision number in pure oxygen, Z is the number of collisions needed to produce a 1/e approach to vibrational equilibrium. The points are ○ Shields and Lee[20], ● Henderson[21], □ Holmes, Smith, and Tempest[22], ■ Knötzel[23], △ Parker[24], and ▲ Blackman[25].

---

[18] L. Landau and E. Teller, Physik Z. Sowjetunion 10, 34 (1938).

[19] F. D. Shields, J. Acoust. Soc. Am. 34, 271 (1962), 32, 180 (1960); 31, 248 (1959); 29, 450 (1957); 29, 410 (1957).

[20] _____, and Kun Pal Lee, J. Acoust. Soc. Am. 35, 251 (1963).

[21] M. C. Henderson, J. Acoust. Soc. Am. 34, 349 (1962).

[22] R. Holmes, F. A. Smith and W. Tempest, Proc. Phys. Soc. 81, 311 (1963).

[23] H. Knötzel and L. Knötzel, Ann. Phys. 2, 393 (1948).

[24] J. G. Parker, J. Chem. Phys. 34, 1763 (1961).

[25] V. H. Blackman, J. Fluid Mech. 1, 61 (1956).

Statement of Problem

This paper describes the design and construction of an apparatus with which to measure the vibrational relaxation time of oxygen in the 300°K to 1300°K range. It is apparent, from the above discussion, that this temperature range for oxygen has not received adequate experimental coverage. This apparatus, designed especially for oxygen, will also be useful in the study of vibrational relaxation times for many other gases.

Parker's[26] approach is followed but with the necessary modifications for a wider temperature and pressure range being made. The apparatus consists of a hollow circular stainless steel cylinder having rigid walls and closed at one end with a piston which vibrates sinusodially thus producing sound waves in the gas contained by the tube. The other end of the tube is closed rigidly except for a small probe tube leading to a microphone which serves as the receiving element. This stainless steel cylinder along with an oven, a gas handling system and the necessary electronic gear are combined in such a manner that sound velocities and sound absorptions can be measured at many different temperatures and pressures.

---

[26] J. G. Parker, J. Chem. Phys. 34, 1763 (1961).

CHAPTER II

THEORY

A. Introduction:

Since the resonance tube has been chosen as the instrument in which to measure the absorption of sound energy, a discussion of what a resonance tube is and the theory of its operation is needed. This chapter, Part B, describes the resonance tube and follows Parker's[1] approach to the use of the tube for the determination of the relaxation time of a gas. The width of a resonance peak, δ, is shown to be proportional to the absorption coefficient, σ, and proportional to the square root of the frequency, f; changes in σ are then related to the relaxation time τ.

A resonance peak occurs each time the frequency of the sound introduced into one end of the tube is such that the reflected wave from the other end of the tube returns in phase with the introduced sound. In this work the resonance peaks (sound pressure maximas) are located by varying the frequency of the "speaker" until a maximum output from the microphone is observed on a voltmeter. The frequency at which this maximum occurs is called f_n where n represents the number of the resonance peak. The width, δ, of the resonance peak in cycles per second is measured at some convenient distance below its maximum. This width

---

[1] J. G. Parker, J. Chem. Phys. 34, 1763 (1961).

is then used in the determination of the relaxation time as outlined in Part D of this chapter. Part C presents a method of reducing the experimental data to give the relaxation time and Part E explains how to calculate sound energy losses in a resonance tube due to wall effects.

B. Relaxation Time From Sound Absorption Measurements:

An ideal acoustic resonance tube, consists of a hollow circular cylinder having infinitely rigid walls with an inflexible piston closing one end and a perfect reflector the other. The piston is driven sinusoidally to and fro in the direction of the tube axis, the x axis, and the plane sound waves thus generated travel down the tube, strike the reflector, reverse direction and finally return to the piston. If the phase of the wave when it returns is equal to that at initiation, a system of standing waves is generated. The condition to be satisfied for the production of these standing waves is that an integral number of half wavelength, $\frac{\lambda_n}{2}$, be contained in the tube of length l', i.e.,

$$l' = \frac{n\lambda_n}{2}; \quad n = 1,2,3... \tag{1}$$

or, in terms of frequency, since $c = f_n\lambda_n$ and $f_a = \frac{c}{2l'}$,

$$f_n = n\,\frac{c}{2l'} = n\,f_a \tag{2}$$

where f_a is the fundamental frequency and c is the velocity of sound in the gas contained by the tube.

Beranek[2] shows that if U is the amplitude of the velocity with which

---

[2]L. L. Beranek, Acoustics (McGraw-Hill Book Co., Inc., N. Y., Toronto, London, 1954) pp. 28-35.

the piston is driven, then the sound pressure within the tube is

$$P(x,t) = -j\rho_o cU \frac{\cos k(l'-x)}{\sin kl'} e^{j\omega t} = -jP_e e^{j\omega t} \tag{3}$$

where $\omega = 2\pi f$, $k = \omega/c$ and $P_e = \rho_o cU \frac{\cos k(l'-x)}{\sin kl'}$. P_e is the maximum amplitude of the extra pressure in the gas due to the sound wave. ρ_o is the density of the gas through which the sound is traveling and $j = \sqrt{-1}$.

In equation (3), under conditions of frequency for which $\sin kl'$ vanishes, P becomes infinite, corresponding to the situation already noted in Equations (1) and (2) i.e., $kl' = n\pi$. This, however, holds only for a dissipationless medium, which is an idealization; nevertheless, it happens under certain circumstances that the dissipation is rather small and in these cases the sound field within the tube can become very large.

From Equation (3) the sound pressure maximum at the reflector, $x = l'$, and $\cos k(l'-x) = 1$, is given by,

$$P_e = \frac{\rho_o cU}{\sin kl'} \tag{4}$$

which, when k is considered complex, i.e.,

$$k = \beta - j\sigma, \tag{5}$$

to account for dissipation, may be written by use of the trigonometric identity, $\sin(A-B) = \sin A \cos B - \cos A \sin B$, and the facts that $\sin jx = j \sinh x$, $\cos jx = \cosh x$ and $\left|P_e\right| = \sqrt{(\text{Real})^2 + (\text{Imag})^2}$

$$\left|P_e\right| = \frac{\rho_o cU}{(\sin^2 \beta l' \cosh^2 \sigma l' + \cos^2 \beta l' \sinh^2 \sigma l')^{\frac{1}{2}}}. \tag{6}$$

In the vicinity of the nth resonance, the real part of kl' becomes by use of the relations $k = \frac{\omega}{c}$ and $\frac{2\pi l'}{c} f_n = n\pi$,

$$\beta l' = \frac{2\pi f}{c} l' = \frac{2\pi l'}{c} (f-f_n) + n\pi \tag{7}$$

and with $\sigma l' \ll 1$ (i.e., small absorption) along with

$$\frac{2\pi l'}{c} (f-f_n) \ll 1, \tag{8}$$

and the small angle approximations, $\sinh^2 \sigma l' \cong (\sigma l')^2$, $\cosh^2 \sigma l' \cong 1$, $\cos^2 \beta l' = \cos^2 \frac{2\pi l'}{c} (f-f_n) \cong 1$ and $\sin^2 \beta l' = \sin^2 \frac{2\pi l'}{c} (f-f_n) \cong \left[\frac{2\pi l'}{c} (f-f_n)\right]^2$ the absolute sound pressure at the reflector for the nth resonance becomes

$$\left|P_{en}\right| = \frac{\rho_o c^2 U}{2\pi l'} \left[\frac{1}{(f-f_n)^2 + (\frac{\sigma c}{2\pi})^2}\right]^{\frac{1}{2}}. \tag{9}$$

This is a bell shaped curve disposed symmetrically about the resonant frequency with a width varying directly as the magnitude of σ. Equation (9) may be further written as

$$\frac{\left|P_{en}\right|}{\left|P_{en}\right|_{max}} = \left\{\left[(\frac{2\pi}{\sigma c})(f-f_n)\right]^2 + 1\right\}^{-\frac{1}{2}} \tag{10}$$

Where $\left|P_{en}\right|_{max}$ is the pressure at reflector when $\sigma = 0$. The two frequencies for which this ratio falls to $\sqrt{\frac{1}{2}}$ are called the "half-power points" and lie at equal distances (number of cycles per second) above and below the point of resonance. Setting Equation (10) equal to $\sqrt{\frac{1}{2}}$ and solving for δ, the frequency separation of these power points, gives

$$\delta = \frac{\sigma c}{\pi} \tag{11}$$

Thus, the sound absorption in the gas may be directly determined from a measurement of δ. By use of Equation (10) and $x = 20 \log \frac{\left|P_{en}\right|_{max}}{\left|P_{en}\right|}$, $\delta = \frac{1.5\sigma c}{\pi}$ when $x = 5$ db and $\delta = \frac{3\sigma c}{\pi}$ when $x = 10$ db.

Concerning the approximations leading to Equation (11), within the half-power frequencies, the inequality (8) is satisfied as long as $\sigma l' \ll 1$ or conversely, $\sigma l' \ll 1$ as long as

$$\frac{2l'}{c}\,\delta \ll 2/\pi$$

which from Equation (2) means that

$$\frac{\delta}{f_a} \ll \frac{2}{\pi}\ .$$

Thus, Equation (11) is valid as long as the width of the resonance curve in cps is much smaller than the fundamental frequency.

Sound absorption within the tube may arise in three different ways. The first is a result of the effects of viscosity and heat conductivity in the interaction of the plane sound waves with the walls of the tube. Viscosity causes the wall to exert a frictional drag on the sound wave, with a consequent loss in momentum; heat conductivity, on the other hand, gives rise to a loss in thermal energy. The theory generally accepted as correctly accounting for these losses is that of Helmholtz and Kirchhoff,[3] which gives for the sound absorption per unit length

$$\sigma_w = \left[\frac{(\eta\pi)^{\frac{1}{2}}}{R}\right]\left\{\frac{1}{\gamma^{\frac{1}{2}}} + \left(\frac{k}{\eta c_v}\right)^{\frac{1}{2}}\left[\frac{\gamma-1}{\gamma}\right]\right\}\left(\frac{f}{P_o}\right)^{\frac{1}{2}} \qquad (12)$$

where η is the coefficient of viscosity, k is the coefficient of heat conductivity, γ is the ratio of specific heats, c_v is the specific heat at a constant volume per gram, R is the tube radius, and P_o is the equilibrium pressure. This formula takes into account only losses arising at the cylindrical surfaces of the tube and does not include end effects. End effects according to Parker[4] contribute approximately $\frac{R}{l'}\sigma_w$ to the tube wall absorption, where R is the tube radius and l' is its length.

---

[3] Lord Rayleigh, Theory of Sound (Dover Publication, New York, 1945), Chapter XIX.

[4] J. G. Parker, J. Chem. Phys. 34, 1763 (1961).

Viscosity and heat conduction also may cause a loss in the body of the gas independent of the boundaries. For this type of loss, the resultant coefficient of absorption is, according to Stokes and Kirchhoff,[5]

$$\sigma_b = \left(\frac{2\pi^2\eta}{c}\right)\left\{\frac{4}{3} + \left[\frac{\gamma-1}{\gamma}\right]\left(\frac{k}{\eta c_v}\right)\right\}\left(\frac{f^2}{P_o}\right) \tag{13}$$

In general, the volume effects of viscosity and heat conductivity are small except at rather high frequencies; so small compared to σ_w that they may be ignored in the audible range.

Thirdly, absorption of energy may take place due to a difference in the rate of approach to equilibrium of the internal degrees of freedom compared to the translational degrees whenever the state of the gas is changed. In general, the rotational degrees of freedom reach equilibrium very quickly (i.e., in less than 10 collisions), however, vibrational degrees may require under certain conditions as many as 10^6 or more collisions. Thus vibration, in general, exhibits a very large dynamic separation from the other degrees of freedom.

The absorption occurring in such a process may be written[6]

$$\sigma_v = \left(\frac{\pi c}{c_o^2}\right)\left[\frac{RC_i}{C_p C_v^o}\right]\left[f_o f^2/(f_o^2 + f^2)\right] . \tag{14}$$

Here c_o is the limiting sound velocity for frequencies sufficiently low that the internal degree of freedom under consideration participates fully, C_i is the specific heat of the internal degree of freedom, C_v^o is the specific heat at constant volume including C_i, i.e.,

---

[5] K. F. Herzfeld, Thermodynamics and the Physics of Matter, (Princeton University Press, Princeton, New Jersey, 1955) Vol. 1, Sec. H.

[6] Ibid.

$$C_v^o = C_v^\infty + C_i,$$

and $C_p^\infty = C_v^\infty + R$ is the specific heat at constant pressure excluding C_i. The quantity f_o is called the relaxation frequency and is related to the relaxation time τ by the relation

$$f_o = \frac{1}{2\pi\tau}\left[\frac{C_p^o}{C_p^\infty}\right]. \tag{15}$$

For oxygen at room temperature, $C_i \ll C_v^\infty$, and Equations (14) and (15) may be written

$$\sigma_v = \left(\frac{\pi}{c}\right)\left[\frac{RC_i}{C_p^\infty C_v^\infty}\right]\left[\frac{f_o f^2}{(f_o^2 + f^2)}\right] \tag{16}$$

also

$$f_o = \frac{1}{2\pi\tau}. \tag{17}$$

Dealing with relatively low frequencies thus small absorptions the total absorption may be written as the sum of the individual contributions, i.e.,

$$\sigma = \sigma_w + \sigma_v.$$

Thus, by Equation (11)

$$\delta = \frac{c\sigma}{\pi} = \delta_w + \delta_v \tag{19}$$

and from Equation (16)

$$\delta_v = \frac{RC_i}{C_p^\infty C_v^\infty}\left[\frac{f_o f^2}{(f_o^2 + f^2)}\right]. \tag{20}$$

C. Reduction of Absorption Data:

Plotting $\frac{f^2}{\delta_v}$ as a function of f^2, according to Equation (20), should

give a straight line with a slope

$$S = \frac{C_p^{\infty} C_v^{\infty}}{RC_i}\left(\frac{1}{f_o}\right) \tag{21}$$

and a zero intercept

$$I = \frac{C_p^{\infty} C_v^{\infty}}{RC_i}(f_o). \tag{22}$$

Combining Equations (21) and (22), gives

$$f_o = \left(\frac{S}{I}\right)^{-\frac{1}{2}}, \tag{23}$$

and by use of Equation (17) the relaxation time is determined, i.e.,

$$\tau = \frac{1}{2\pi}\left(\frac{I}{S}\right)^{-\frac{1}{2}} \tag{24}$$

where the intercept, I, and the slope, S, are read from the $\frac{f^2}{\delta_v}$ versus f^2 curve.

D. Procedure for Collecting and Reducing Data:

The preceding absorption theory is applied to the determination of the relaxation time of a gas by the following procedure. The steps in this procedure consist of a--

1. determination of δ_w (experimental) as a function of frequency, f, with a nonrelaxing gas;
2. calculation of δ_w (theoretical) by use of Equations (11) and (12) for the nonrelaxing gas used in Step 1;
3. calculation of the per cent deviation of δ_w (experimental) from δ_w (theoretical) found in Steps 1 and 2;
4. determination of δ (experimental) as a function of frequency for the relaxing gas;
5. calculation of δ_w (theoretical) for the relaxing gas by use of Equations (11) and (12);

6. correction of δ_w (theoretical) for the relaxing gas by the per cent deviation found in Step 3, thus giving δ_w (corrected) for the relaxing gas;

7. calculation using Equation (19) to determine δ_v for the relaxing gas, i.e.,

$$\delta_v = \delta \text{ (experimental)} - \delta_w \text{ (corrected)};$$

8. plotting of $\frac{f^2}{\delta_v}$ as a function of f^2 to give a curve from which the slope, S, and intercept, I, are measured; and

9. calculation of the relaxation time by use of Equation (24).

The apparatus designed in this paper is calibrated according to Steps 1, 2, and 3 above. The data for this calibration are in Chapter IV.

E. Method of Calculating σ_w:

In order to calculate δ_w (theoretical), Step 2 in the above procedure, Equation (12) must be solved. The following discussion illustrates a method of solving for σ_w (theoretical) at different temperatures, then by use of Equation (11), δ_w (theoretical) may be calculated.

For an ideal gas the expression for tube absorption is given by Equation (12). In this case the classical absorption is small in comparison to the tube absorption. For a given gas, Equation (12) can be put in the form

$$\sigma_w = \frac{k_t}{8.686}\left(\frac{f}{P_o}\right)^{\frac{1}{2}}, \ (\text{cm})^{-1} \tag{25}$$

where

$$k_t = \frac{(\pi\mathfrak{M})^{\frac{1}{2}}}{R}\left[\frac{1}{\gamma^{\frac{1}{2}}} + \left(\frac{\gamma-1}{\gamma}\right)\left(\frac{k}{c_v\mathfrak{M}}\right)^{\frac{1}{2}}\right] \tag{26}$$

and k_t is a function of temperature. The variation of k_t with temperature

for nitrogen is shown in Figure 2 which is a plot of data given in Table I. These values are taken from Shields and Lagemann[7] and adjusted to fit a tube of 2.466 cm. radius instead of their smaller tube of 0.865 cm. radius.

TABLE I

ABSORPTION IN NITROGEN AT VARIOUS TEMPERATURES

Temperature degrees C	k_t, calculated from Equation (26)
-0.1	0.086
25.6	0.089
51.0	0.092
99.9	0.097
151.4	0.101

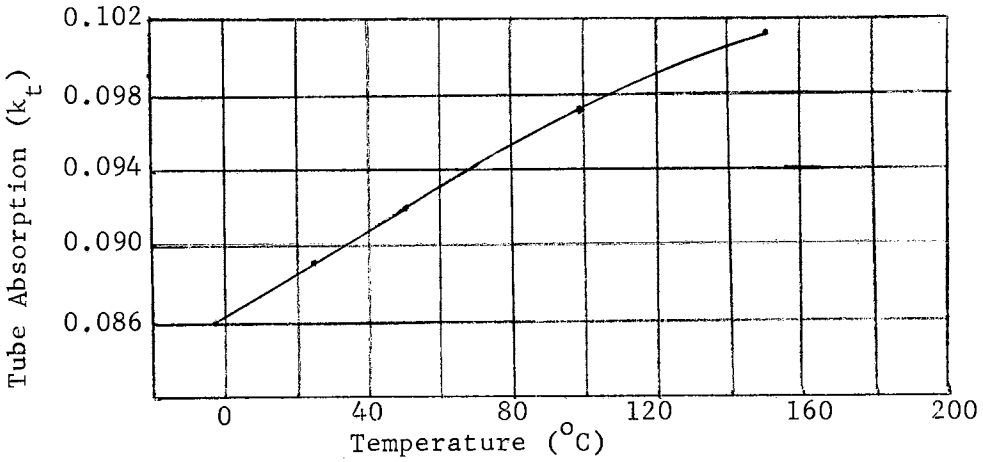

Figure 2. Dependence of the tube absorption (k_t) on temperature for nitrogen as calculated from Kirchhoff's equation.

[7] F. Douglas Shields and Robter T. Lagemann, J. Acoust. Soc. of Am. 29, (470), 1959.

The units of k_t in Figure 2 are such that σ_w is in decibels/centimeter (intensity attenuation) when f is in kilocycles per second and P is millimeters of mercury, i.e., k_t has the units decibels per cm./(kilocycles per sec per mm Hg)$^{\frac{1}{2}}$. Equation (25) is written so that σ_w will have a dimension of $(cm)^{-1}$.

CHAPTER III

THE DESIGN OF AN ACOUSTIC INSTRUMENT

An acoustic instrument with which to measure sound absorption and velocity in gases over a wide range of both temperature and pressure is needed. After a search of the literature, it was decided that Parker's[1] Kundt tube technique could be used, provided the speaker and microphone were removed from the heated region; or that, possibly, a speaker and microphone could be designed to operate at the high temperatures and pressures. The latter approach was followed until the problem of designing a high temperature speaker and microphone became too time consuming for inclusion in the overall problem.

A goal of approximately 900°C and 50 atmospheres was set for temperature and pressure maximas with an oxygen atmosphere. This goal determined the materials, to a great extent, from which the resonance tube was built.

For construction of the tube and components, stainless steel 304 was chosen from the available heat resisting alloys because of its resistance to oxidation at high temperatures. Properties of stainless steel 304 are listed in Appendix A, as given in the April, 1963 "Steel Products Manual."

---

[1] J. G. Parker, J. Chem. Phys. 34, 1763 (1961).

A. Resonance Tube:

The resonance tube used is made of stainless steel 304 and has an inner diameter of 1.943 ± 0.001 in., a wall thickness of .216 in., and a length of 38 in. Figure 3 is a photograph of the tube showing the 4.375 inch flange at each end to which the driver and microphone assemblies are to be attached. The inside of this tube is honed to a mirror finish with a 0.0001 eccentricity. The two ends are grooved to receive Parker 2-135 O-rings for sealing against vacuum and pressure leaks. At temperatures above about 250°C, United metallic O-rings are to be used.

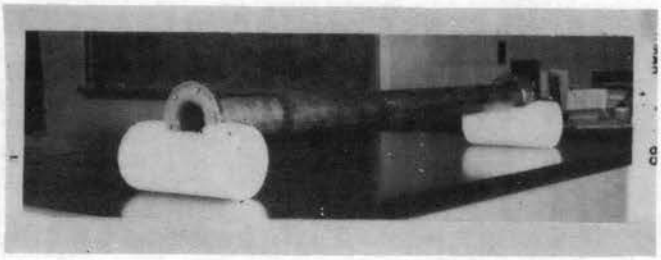

Figure 3. Resonance Tube

B. Driver Assembly:

The driver assembly design is shown in Figure 4. This design was decided upon after extensive experimental work with conventional speakers. The temperature and pressure requirements along with an oxygen atmosphere prevented the use of a conventional speaker directly inside the resonance tube.

The driver consists of a 1 inch thick by 4.375 inch circular solid cylinder of stainless steel machined to take a specially designed bellows shown in Figure 5. A piston is attached to one side of the bellows and a Goodman Vibration Generator Type V-47 by way of a shaft is attached

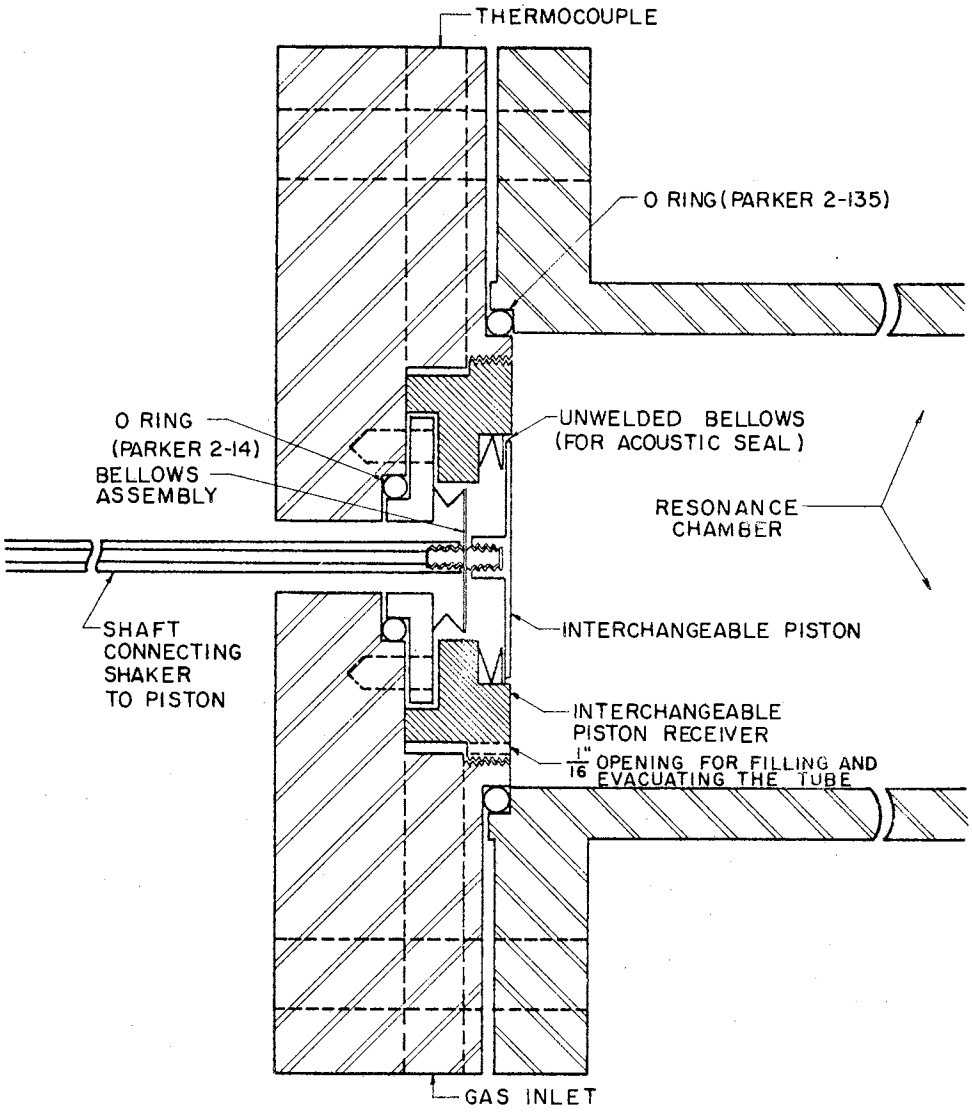

Figure 4. Driver assembly, showing the 1 inch by 4.375 inch stainless steel body with the inconel bellows attached. A Conax thermocouple fitting is to be mounted as shown, opposite the gas inlet tube. An interchangeable piston receiver is provided in order to determine the optimum piston design. The unwelded "bellows" is to prevent radiations off the backside of the piston from entering the resonance chamber.

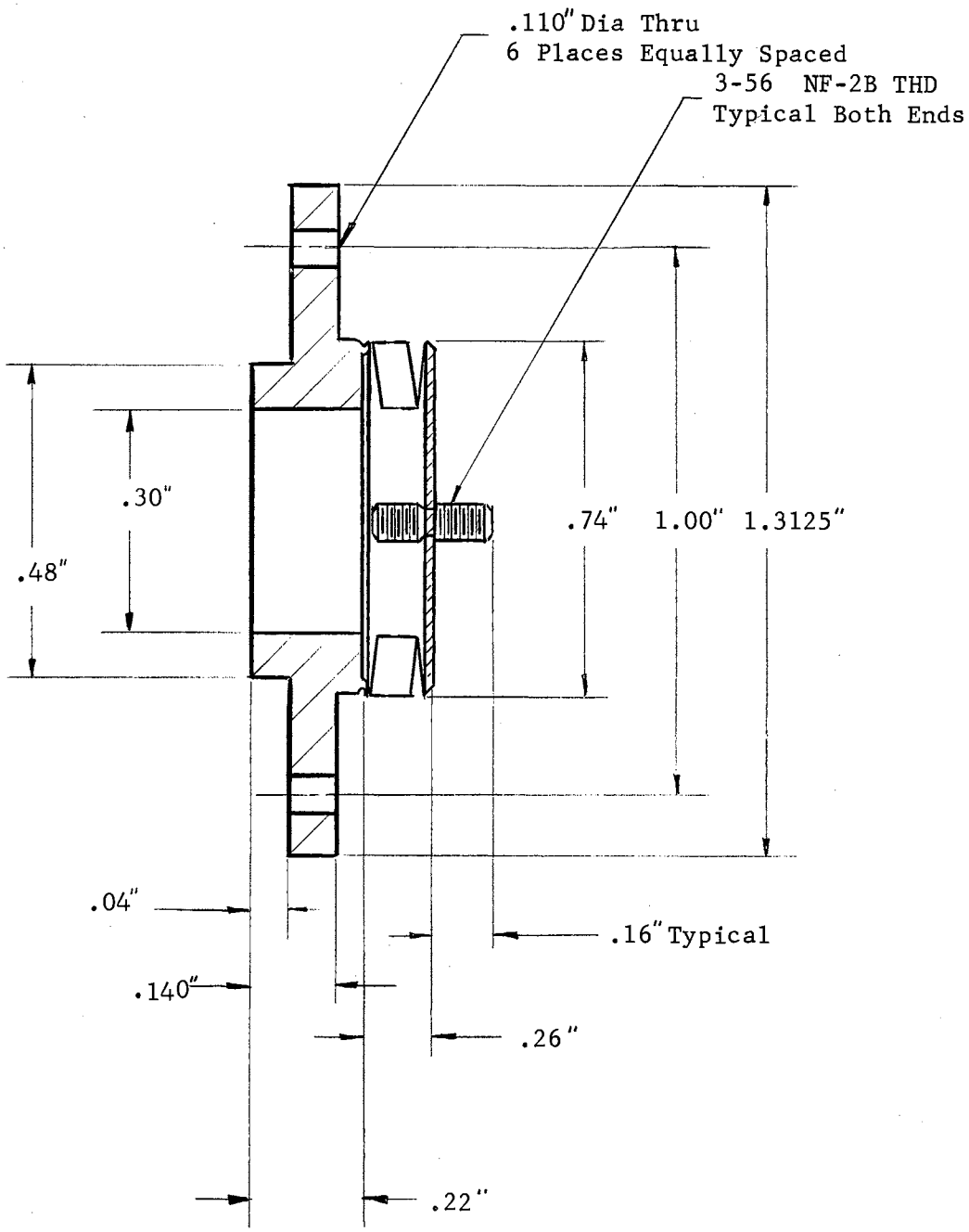

Figure 5. The driver bellows, made of inconel and stainless steel 304 has a spring rate of 1500 pounds per inch and withstands a hot oxygen atmosphere at pressures to 250 pounds per square inch. The bellows is designed to transmit vibrations to 10,000 cycles per second.

to the other. The vibrator moves the piston sinusoidally to produce sound energy. Several pistons were tried until the 1.46 inch diameter x 0.152 inch thick one was determined to give a good response. Performance curves for the vibration generator are shown in Figure 6.

A single gas inlet and evacuation line is attached to the driver assembly. Gases are admitted and removed from the resonance chamber through a 1/16" hole in the piston receiver. A Conax MTG-20-A2 chromel-alumel bare wire thermocouple located inside the driver assembly and whose emf is read as degrees centigrade on a Leeds & Northrup temperature potentiometer, Catalog No. 8692, is used to make temperature measurements on the gas inside the tube.

The bellows shown in Figures 4 and 5 was made by the Metal Bellows Corporation, Chatsworth, California. This bellows, made of inconel and stainless steel 304, has a spring rate of 1500 pounds per square inch and was designed for vibrations to 10,000 cycles per second. It will withstand an oxygen atmosphere at high temperatures and pressures to 250 pounds per square inch. Higher pressures will not rupture the bellows but will collapse it thus making the driven piston inoperative. See Figure 5 for the bellows design.

C. Mike Assembly:

Figure 7 is a photograph of the microphone assembly. This assembly consists of an Altec Lansing 21BR 150-3 condenser microphone enclosed in a vacuum tight chamber with cooling jacket attached. The microphone will operate at temperatures to 500^{o}F but the preamplifier must be kept below 212^{o}F.

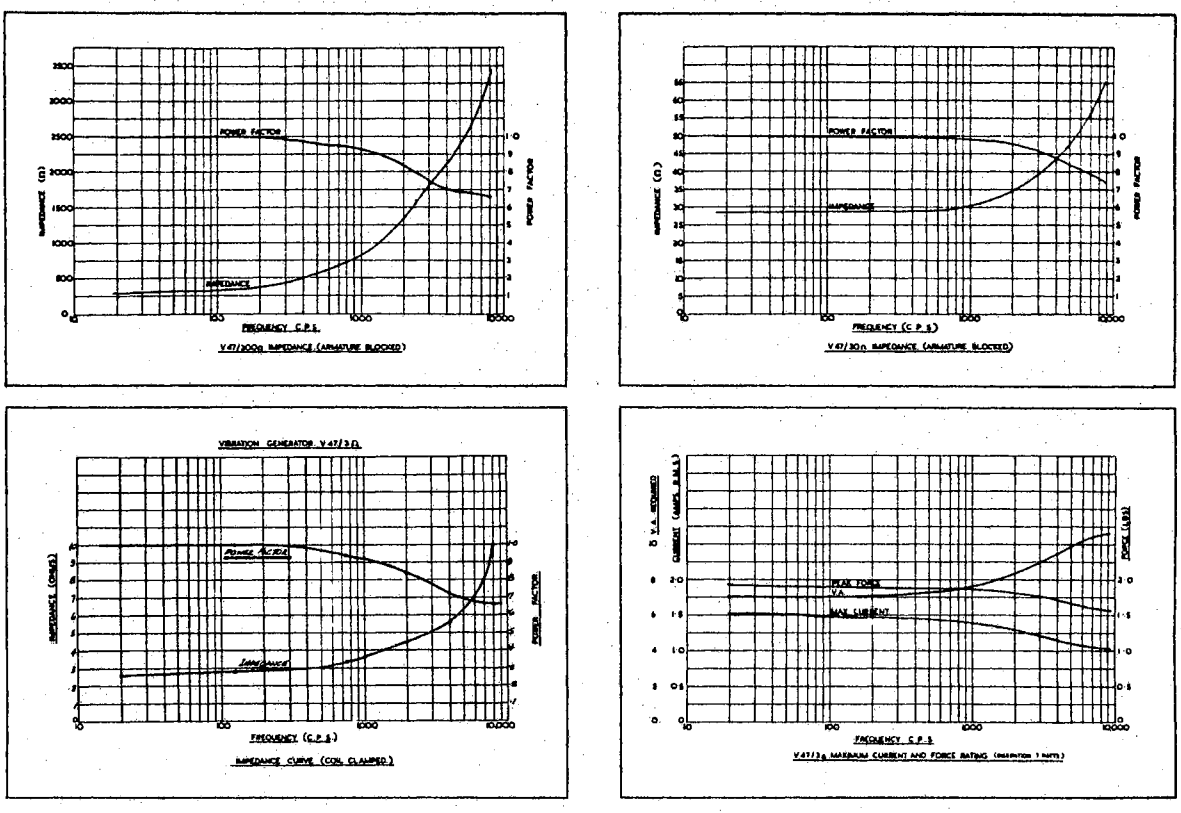

Static Force Factor (lb/A)	0.9
Maximum Continuous Current (D.C. to 500 c/s) (A.r.s.m.)	1.5 (3-ohm model)
D.C. Resistance (ohms)	2.5 (standard)
Impedance at 500 c/s (ohms)	3.0 standard 30 for pick-up use 300 to special order
Power Requirement	5 vA
Total Stroke (ins)	0.1
*Frequency Limit	10 Kc/s
Fundamental Resonance	120 c/s standard 55 c/s 30-ohm model
Mass of Moving System	6.5 gm
Pick-up Coil:	
Sensitivity for 30-ohm Coil (mV/in/sec)	200
R (ohms) for 30-ohm coil	30
Total Weight	2 lb
Dimensions in inches overall	$2\frac{1}{2} \times 2\frac{1}{4} \times 3\frac{1}{4}$
Driving Spindle (Int. Thread):	6-32 x $\frac{5}{16}$ deep
PEAK THRUST	±2 lb at 1 Kc/s

Useful power can be obtained beyond 10 Kc/s by use of mechanically tuned system.

Figure 6. Specifications of the Goodman V47 Vibration Generator

A low capacity mike lead was needed through which to connect the Altec Lansing preamplifier. An Electrical Industries glass hermetically sealed center terminal, Type 470S-1/075, is used to provide this low, 0.46 μμf, capacity lead; see Figure 8 for the design. Thus, the microphone is inside the resonance tube's atmosphere while the preamplifier is outside but very close to the mike. No change in the microphone's performance due to the addition of the low capacity lead has been detected.

The manufacturer's response curve for the Altec Lansing microphone is shown in Figure 9.

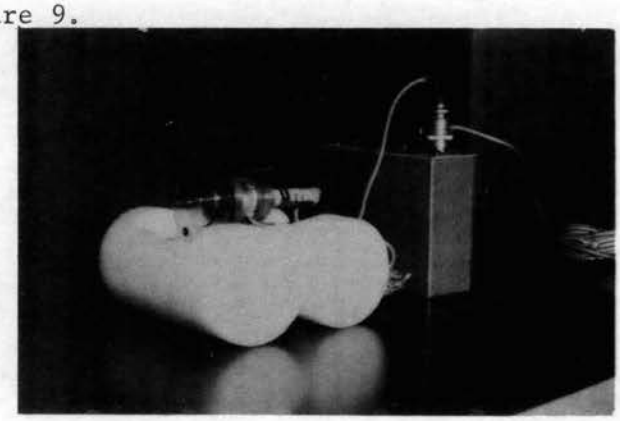

Figure 7. Complete microphone assembly with power supply

D. Gas Handling System:

Photographs showing the gas handling system are shown in Figure 10. Figure 11 is a flow chart of the system. All valves are high pressure Aminco with high pressure fittings. Two Heise oxygen gauges one for pressures from 0 to 5 atmospheres and another for pressures from 0 to 50 atmospheres are used to measure pressures. High pressure tubing is used throughout. Tubing of 5/16 inch I. D. is used in the evacuation circuit while .0875 inch I. D. tubing is used elsewhere. A mercury manometer is attached for use in later work with mixtures of

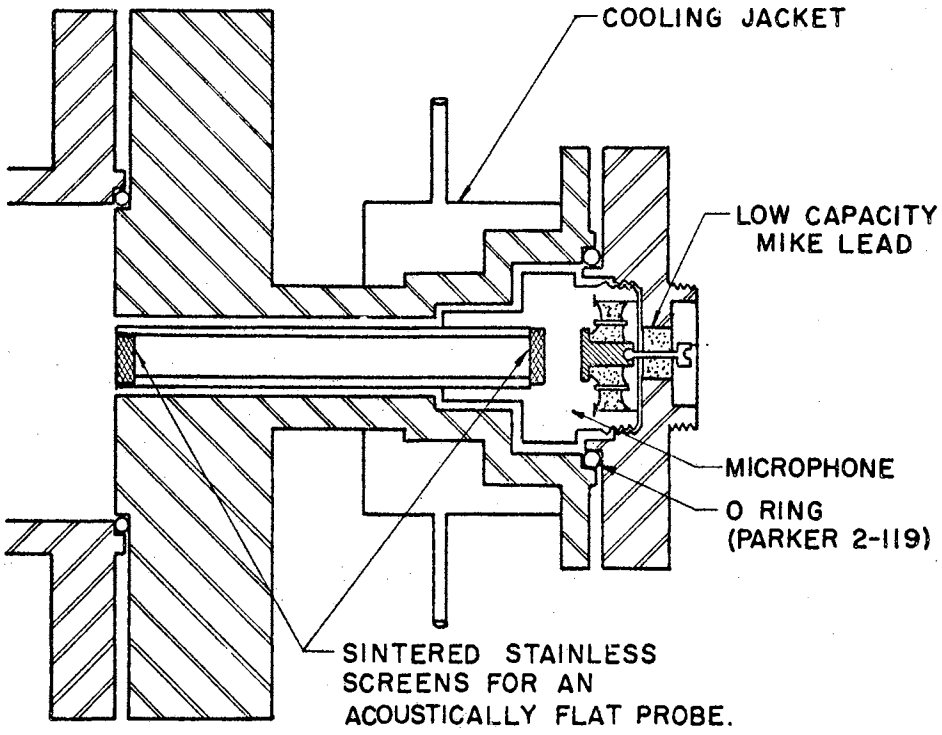

Figure 8. Microphone sound probe assembly, showing the low capacity mike lead and the cooling jacket.

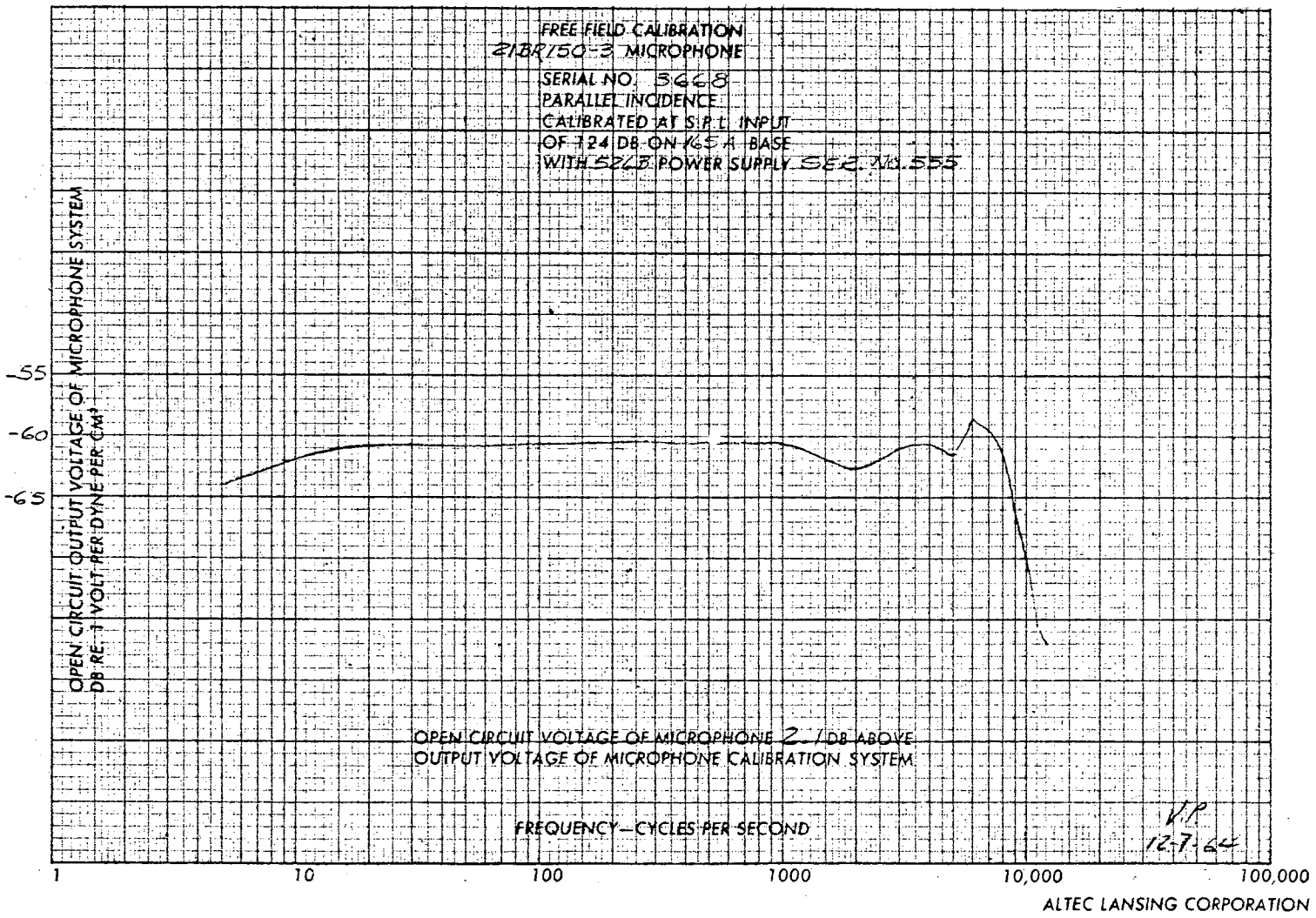

Figure 9. Response Curve for the 21BR 150-3 Microphone

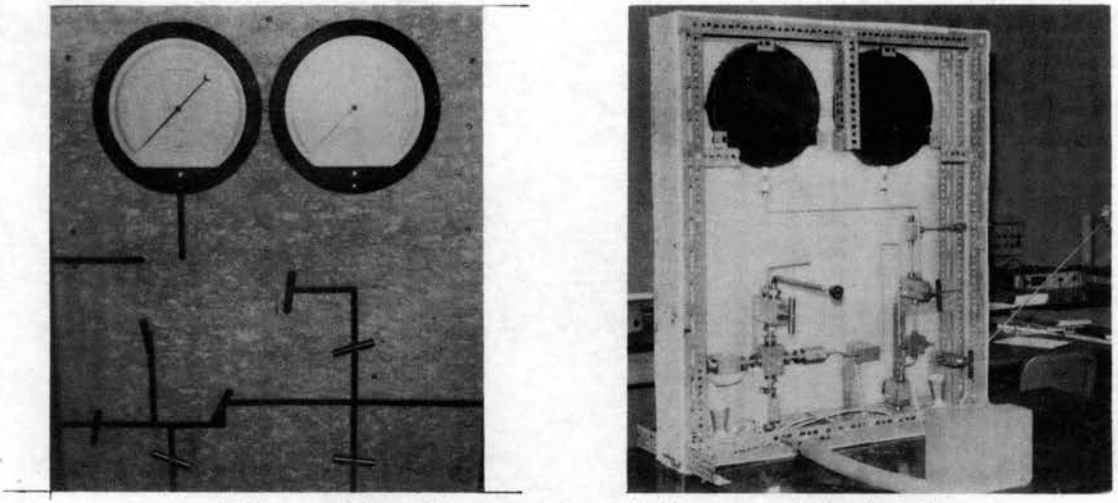

Figure 10. Photographs of front and back of gas handling system. The system is enclosed with asbestos for baking while evacuating.

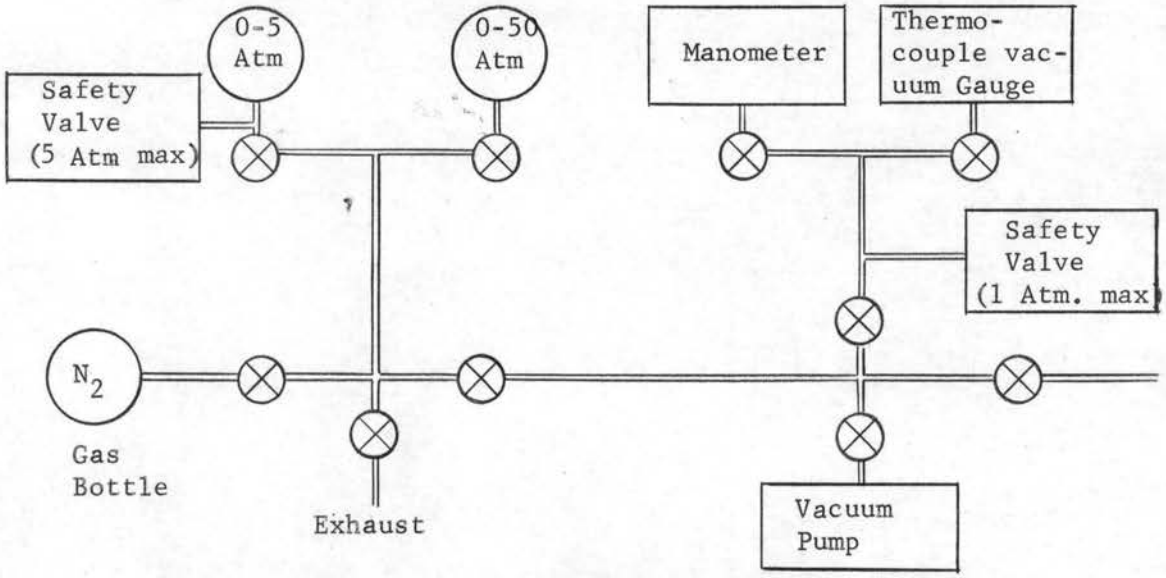

Figure 11. Flow chart of the gas handling system

gases, where it will be used to measure the low pressures of the impurity gases.

Evacuation is achieved by use of a Welch 1402 vacuum pump. The gas handling system can be evacuated to a few tenths of a micron and has a leak of 1 micron per hour. With the resonance tube in place the few tenths of a micron minimum pressure can be attained with a leak rate of 4-5 microns per hour after baking the entire system for several hours. These low pressures are measured with a Consolidated thermocouple vacuum gauge Type GTC-100 with GTC-004 tube. Appendix B contains equations for

calculating the time required to evacuate a known volume.

E. Oven Design and Control:

Figure 12 is a photograph of the oven that is used to heat the resonance tube. This oven is 10 inches square by 43 inches long. The walls are ¼ inch asbestos and are lined with aluminum foil and 2 inches of fiber glass. A five inch square by 41 inch long 16 guage iron liner wrapped with glass insulated heater tapes provides the heated area in which the resonance tube is mounted. The heater tapes are controlled by use of variacs, with a small wattage being controlled with a Barber-Coleman Amplitrol which is set to cycle at the desired temperature. A fan is located inside the oven to smooth temperature gradients which develop. The fan motor is located beneath the table supporting the oven and a long shaft leads from the motor to the fan blades inside the oven. The resonance tube is mounted rigidly to the ¼ inch oven bottom with 1" x 3/10" flat iron clamps. The oven is wired as shown in Figure 13.

Temperature gradients along the resonance tube are checked with several thermocouples making contact with the tube's outside wall. If gradients are found, manually controlled heater elements are adjusted to even the temperature. Some typical performance curves and variac settings are shown in Figure 14.

A comparison of the temperature gradient along the outside of the resonance tube with the temperature gradient inside the tube is shown in Figure 15. This figure indicates that the gas inside has a more uniform temperature than the stainless steel tube, thus small temperature gradients along the outside can be tolerated. In this case, no special effort was made to eliminate the outside temperature gradient. This

accounts for the big fluctuations in the outside temperatures and, yet, the inside temperature shows only a 1.7°C maximum fluctuation.

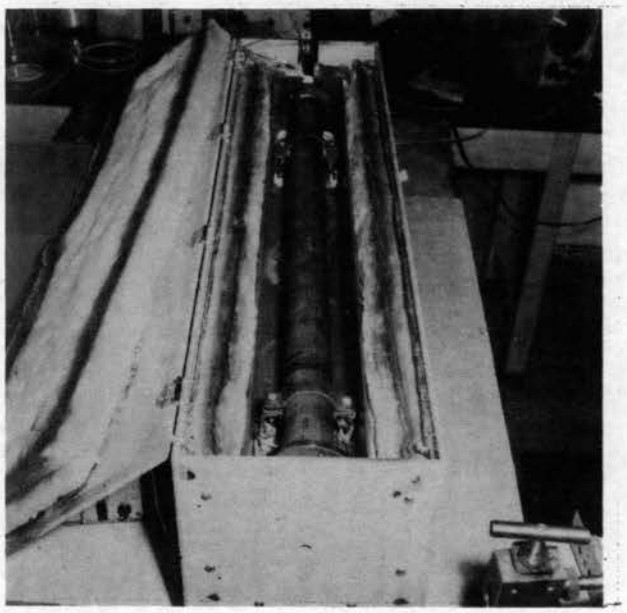

Figure 12. Photograph of the oven with resonance tube in place

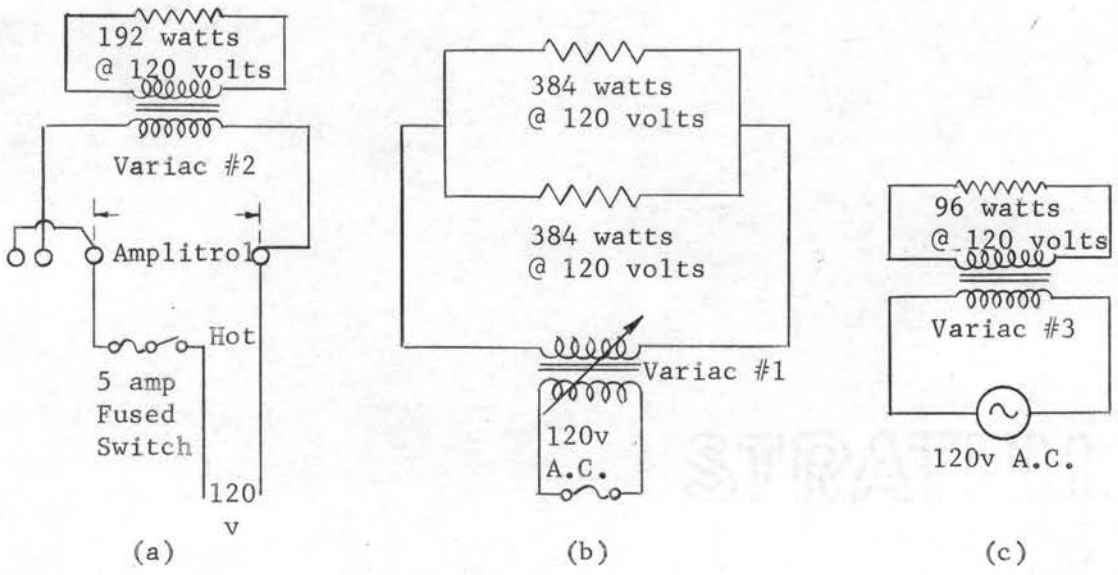

Figure 13 . Oven wiring diagram a. Amplitrol circuit with Variac #2 controlling 192 watt tape along bottom of oven liner b. Variac #1 controlling two 384 watt tapes wrapped around oven liner c. Variac #3 controlling a 96 watt heater tape wrapped around the right end of the resonance tube to supply heat lost to the microphone heat sink.

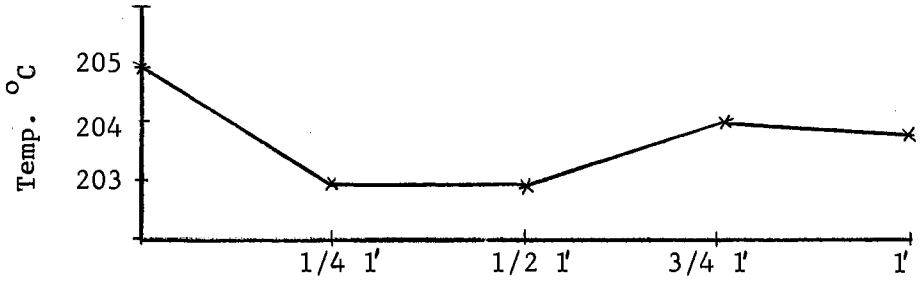

Location of Thermocouples Along Length of Tube, 1'

a. Typical curve showing the temperature gradient along the outside of the resonance tube with the oven controls set as follows--

Amplitrol----200°C;
Variac #1----50 volts;
Variac #2----70 volts;
Variac #3----30 volts;
Fan operating at full speed--60 volts;
Air circulating through mike assembly, temperature inside mike 73.0°C.

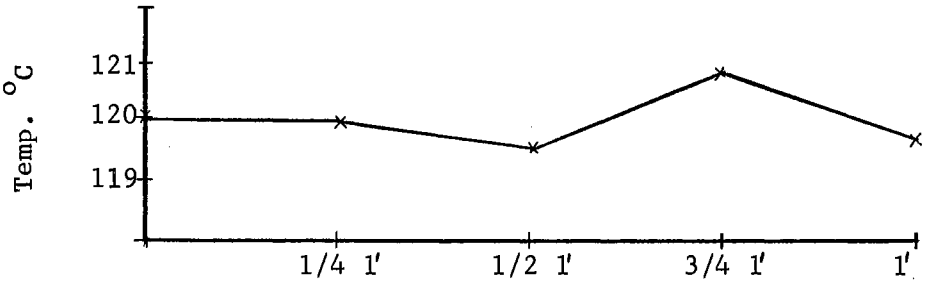

Location of Thermocouples Along Length of Tube, 1'

b. Typical curve showing the temperature gradient along the outside of the resonance tube with the oven controls set as follows--

Amplitrol----120°C;
Variac #2----120 volts;
Variac #3---- 20 volts;
Fan @ 60 volts;
Air circulating through mike assembly, temperature inside mike 50°C.

Figure 14. Typical operating curves for the oven with the settings required to maintain a temperature of (a) 200°C and (b) 120°C. (For 50°C, the amplitrol is set at 50°C and variac #2 at 90 volts.)

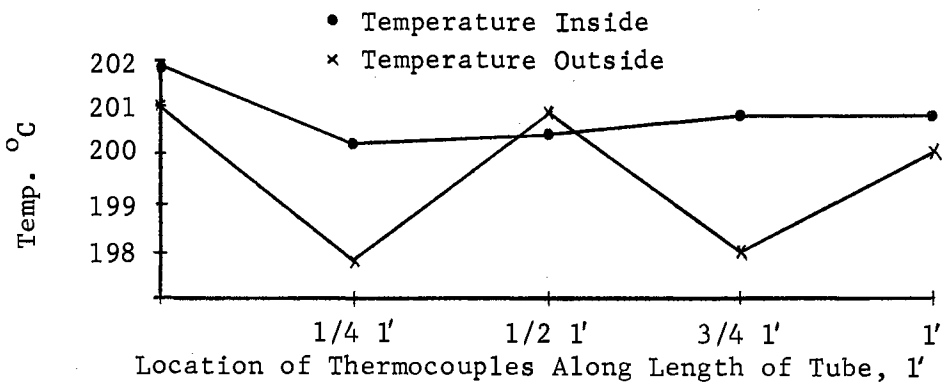

Figure 15. Temperatures of outside of resonance tube compared with temperatures of the enclosed gas

F. Electronic Equipment:

A Brüel and Kjaer Type 1022 Beat Frequency Oscillator is used as a signal generator. This gives good frequency stability and has a fine adjustment adequate for this work. Signals from the oscillator are counted by a Hewlett Packard 5212A counter, and then fed to the Goodman VR47 electromagnetic driver. The output of the Altec Lansing 21-BR 150-3 microphone, which receives the sound transmitted through the gas in the resonance tube, is fed into an Altec Lansing 165A preamplifier powered by an Altec Lansing 526 B power supply, then into a Hewlett Packard Model 400D Vacuum Tube RMS voltmeter by way of a 0.01 μf, 100 Kω filter. A Hewlett Packard Model 130A oscilloscope is used to observe the signal as produced by the microphone. This signal is also recorded on a Brüel and Kjaer Type 2305 Level Recorder. This equipment is arranged as shown in Figure 16. A volt-ohm meter is used to measure the current through the Goodman vibration generator.

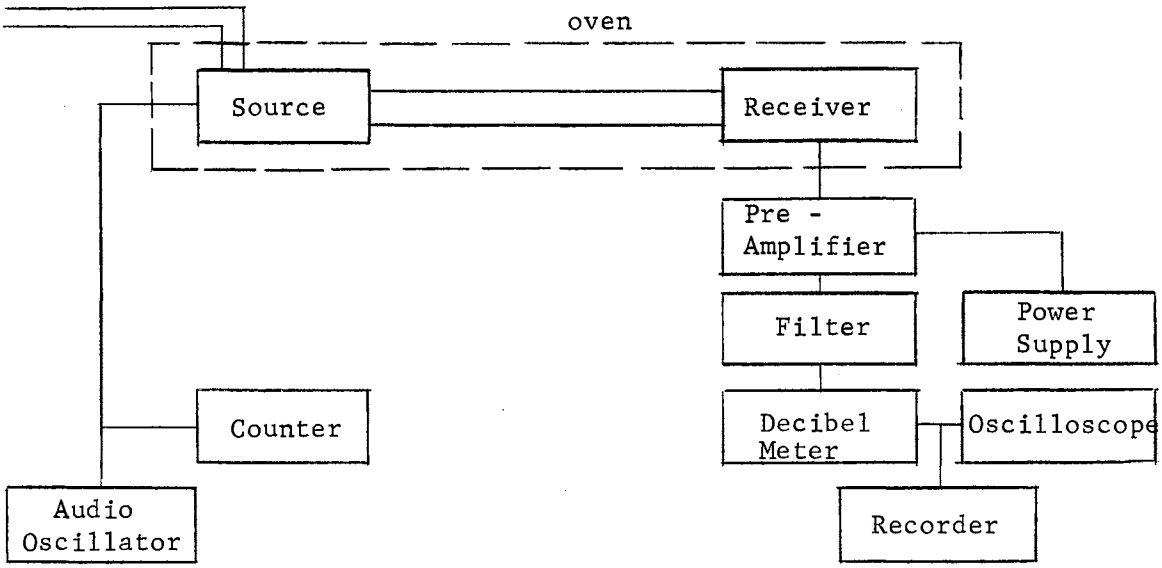

Figure 16. Arrangement of the electronic equipment

CHAPTER IV

TESTING AND CALIBRATING THE APPARATUS

In preparation for a run, the whole system is outgassed for a day or two until the pressure is about 3 microns, with the gas handling system being held at 110°C and the resonance tube about 50°C above the planned operating temperature. The oven temperature is then adjusted to the desired level and gas is admitted to the resonance tube. The system is evacuated again and refilled with more gas. After repeating this filling and pumping procedure a few times, the gas pressure is adjusted to the desired level.

When the temperature and pressure reach their steady state values, the measurement of absorption is started. A nonrelaxing gas is used in the beginning in order to calibrate the tube. Absorption data are analyzed by use of the theory presented in Chapter II and the wall loss determined. This wall loss is compared with the theoretical value as predicted by Equations 11 and 12, Chapter II. By this standardization procedure, the tube is made ready to use with a relaxing gas in which the tube wall loss will account for only part of the total absorption with relaxation accounting for the remainder.

In making a measurement, the driver frequency is varied until resonance is obtained and then the gain of the Brüel and Kjaer oscillator adjusted to give a microphone output sufficient to produce a reading on the vacuum tube voltmeter. The frequency is then varied either side of resonance until the voltmeter reading drops 3db, these frequencies being

recorded along with the resonant frequency. The Hewlett Packard 5212A counter is used to measure the three frequencies.

The combined noise level and level caused by signals transmitted along paths other than the gas column is 30 db or more below the value at resonance except for a few resonant peaks as shown in Figure 17. This figure is a typical recording as produced by the Brüel and Kjaer level recorder. The solid curve is for nitrogen at 60°C and 1.01 atmosphere pressure. The dashed curve shows transmitted noise along the evacuated resonance tube. Both curves were produced with identical settings on all the electronic equipment. The driver had a 0.14 amp current through it. The vacuum tube voltmeter was set at -20 db for the first 4 harmonics and -30 db for the remainder.

After determining the transmitted sound level, the first set of runs was devoted to a determination of absorption in pure nitrogen. A typical set of data is shown in Figure 18, where the resonance width, δ, versus the mode number, n, on a $\sqrt{n}$ scale is plotted. As can be seen in the figure, the variation of δ with $\sqrt{n}$ is approximately linear as predicted by Equations 11 and 12 but the experimental curve misses the origin by about 2 cps. This intercept on the δ axis is not completely understood but is apparently an absorption in addition to that due to the tube walls. The slope of the experimental curve agrees with that predicted by theory which indicates that, with proper calibration, the tube should be useful in detecting extra absorption that would occur in a relaxing gas. Quantitatively this curve is given by

$$\delta_{exp} = 2.01 \sqrt{n} + 2.4$$

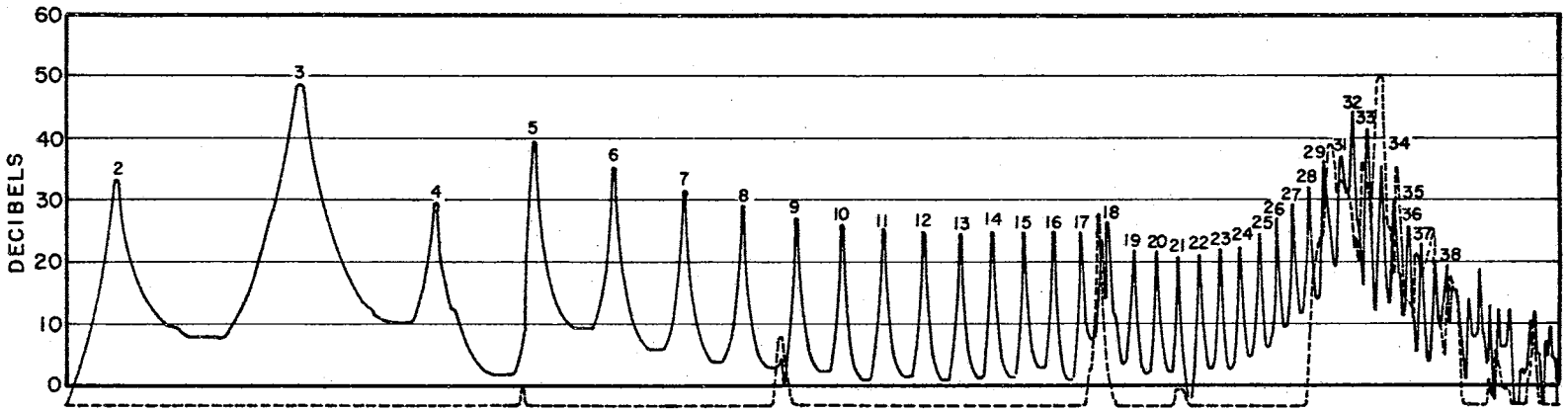

Figure 17. Typical recording of the resonance peaks as produced by the Brüel and Kjaer level recorder. The solid curve is for nitrogen at 60°C and 1.01 atmosphere pressure. The dashed curve shows the transmitted noise level with the resonance tube evacuated to 4 microns pressure. Each division in the vertical direction represents 10 db and the resonance peaks are numbered horizontally. These curves were made with identical settings on all the electronic equipment thus showing where interference from conducted noise occurs. For higher temperatures the conducted noise occurs at approximately the same frequencies as on the above curve but these frequencies represent different resonances due to higher fundamental frequencies at higher temperatures.

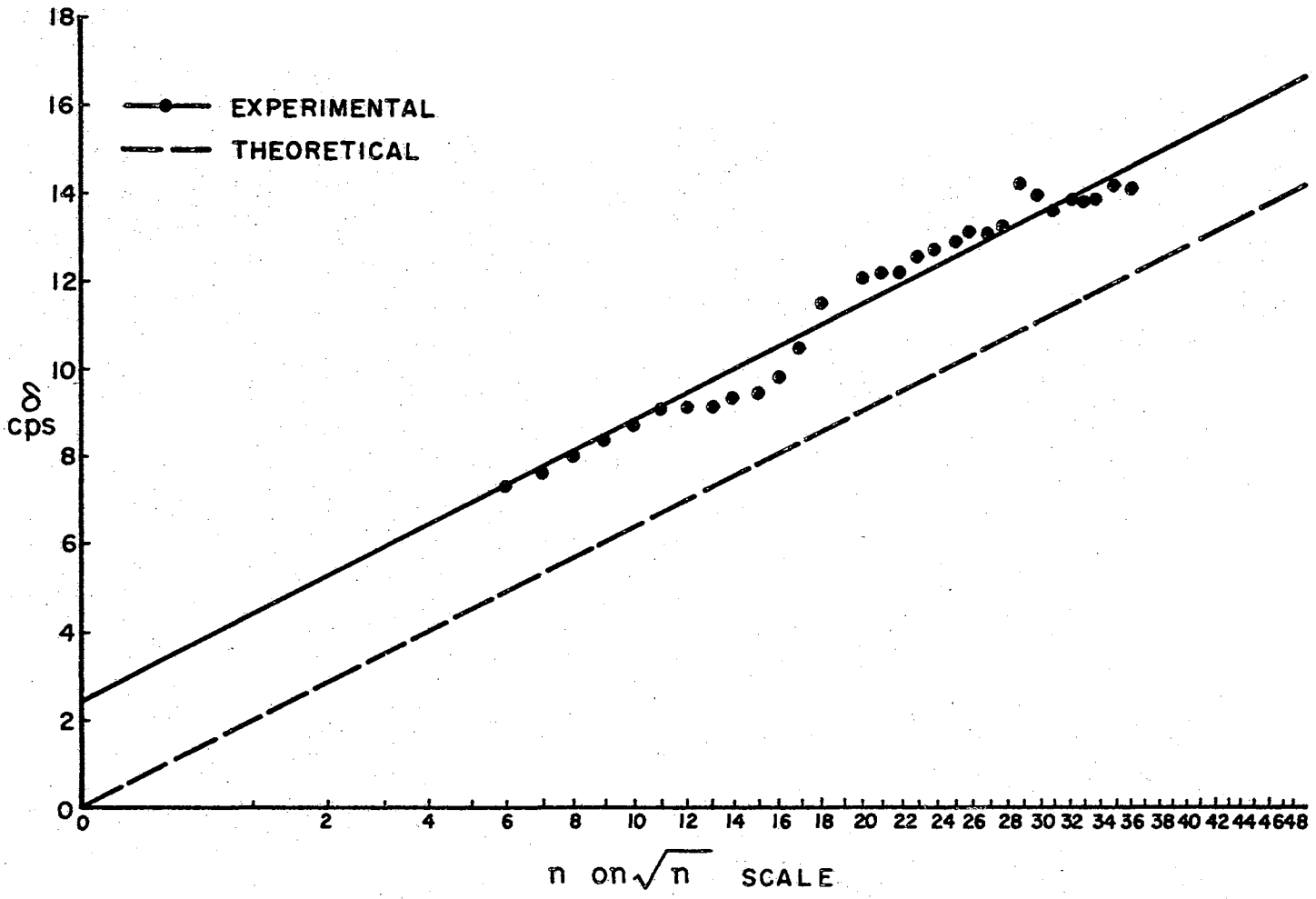

Figure 18. Absorption in nitrogen at 60°C and 1.01 atmosphere absolute, where n is the harmonic number and δ is the width of the resonance peaks, between the half power points.

The broken line in Figure 18 is a plot of the theoretical tube wall absorption in nitorgen as calculated from Equations 11 and 12 and has the equation

$$\delta_{th} = 2.01\sqrt{n}.$$

Thus, the experimental values of δ exceed the theoretical by 2.4 cps.

As is apparent in Figure 18, the experimental points are spread over a wider range than desirable, and possibly the curve could go through the origin. If such a curve is drawn, its slope is 25% greater than the slope of the theoretical curve. Parker[1] found an excess absorption of 19%, Henderson[2] found an excess of 10-15% and Holmes, Smith and Tempest[3] found a 30-40% greater absorption than predicted by wall loss theory. This excess is probably due to end effects and tube walls not being smooth enough. Even with the spread of experimental points, no real justification could be found for drawing the curve through the origin; hence it is drawn with the same slope as the theoretical curve, and this procedure seems to give the best fit. The curves in Figures 19-22 are fitted to the data by this procedure also.

The spread of data becomes worse with increased pressure but the above curve fitting procedure seems satisfactory for all the different temperature-pressure combinations examined thus far. The data being more erratic at higher pressures may be due to the wall loss decrease which allows the other absorption characteristics of the tube to become more

---

[1] J. G. Parker, J. Chem. Phys., 34, 1763 (1961).

[2] M. C. Henderson and G. J. Donnelly, J. Acoust. Soc. Am. 34, 779 (1962)

[3] R. Holmes, F. A. Smith and W. Tempest, Proc. Phys. Soc., 81, 311 (1963).

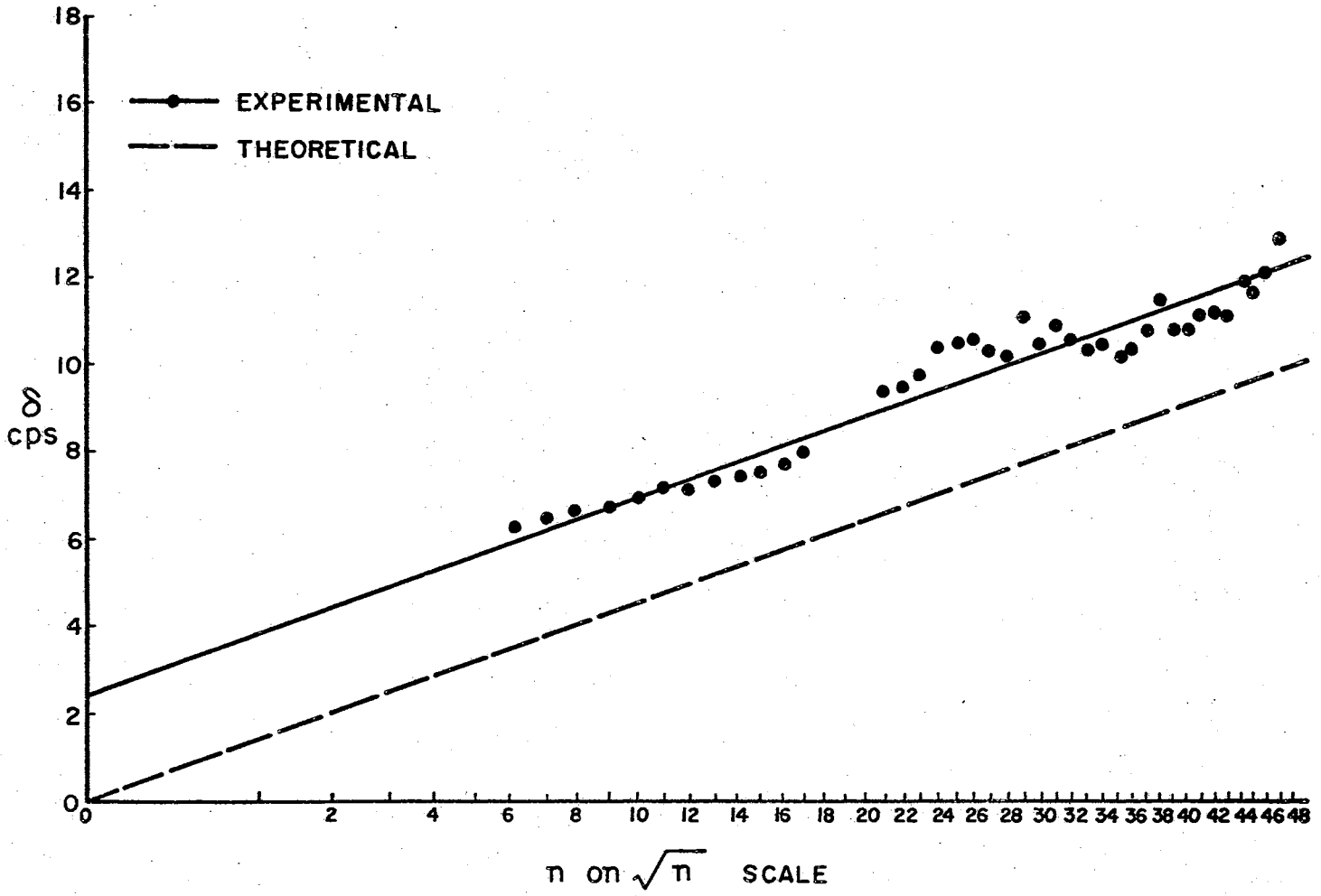

Figure 19. Absorption in nitrogen at 60°C and 2.01 atmospheres absolute, where n is the harmonic number and δ is the width of the resonance peaks, between the half power points

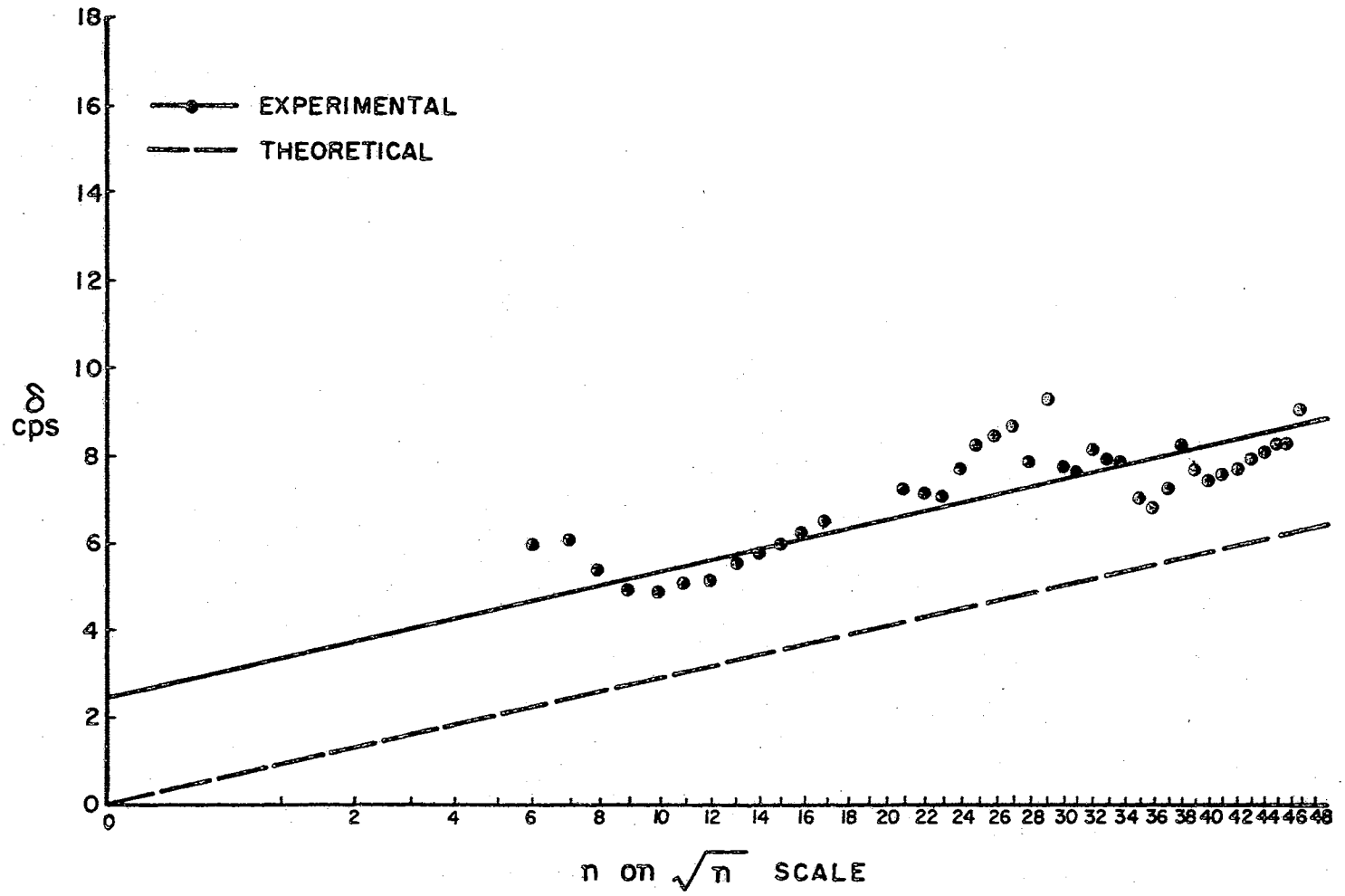

Figure 20. Absorption in nitrogen at 61°C and 5.0 atmospheres absolute, where n is the harmonic number and δ is the width of the resonance peaks, between the half power points

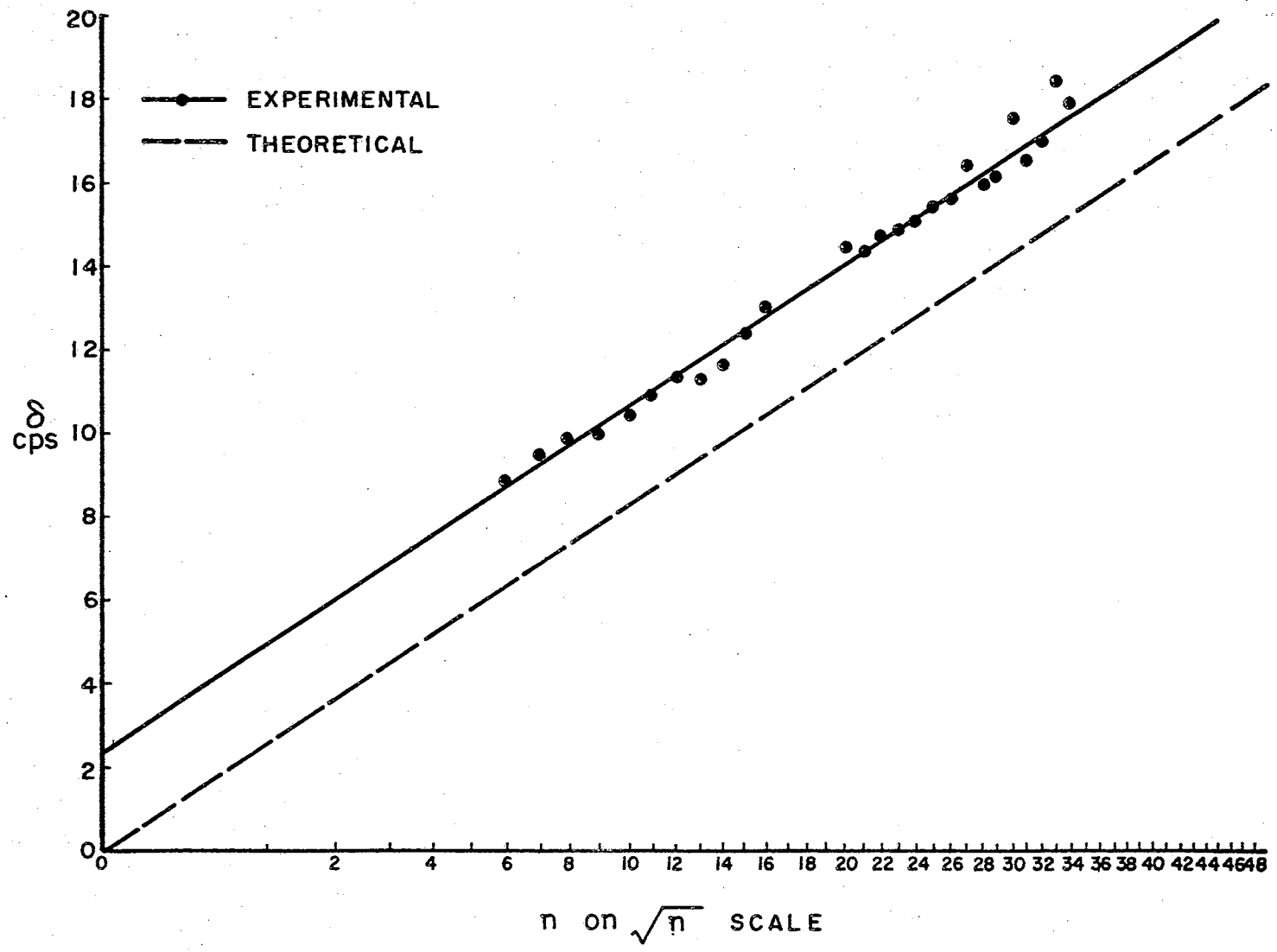

Figure 21. Absorption in nitrogen at 150°C and 1.0 atmosphere absolute, where n is the harmonic number and δ is the width of the resonance peaks, between the half power points

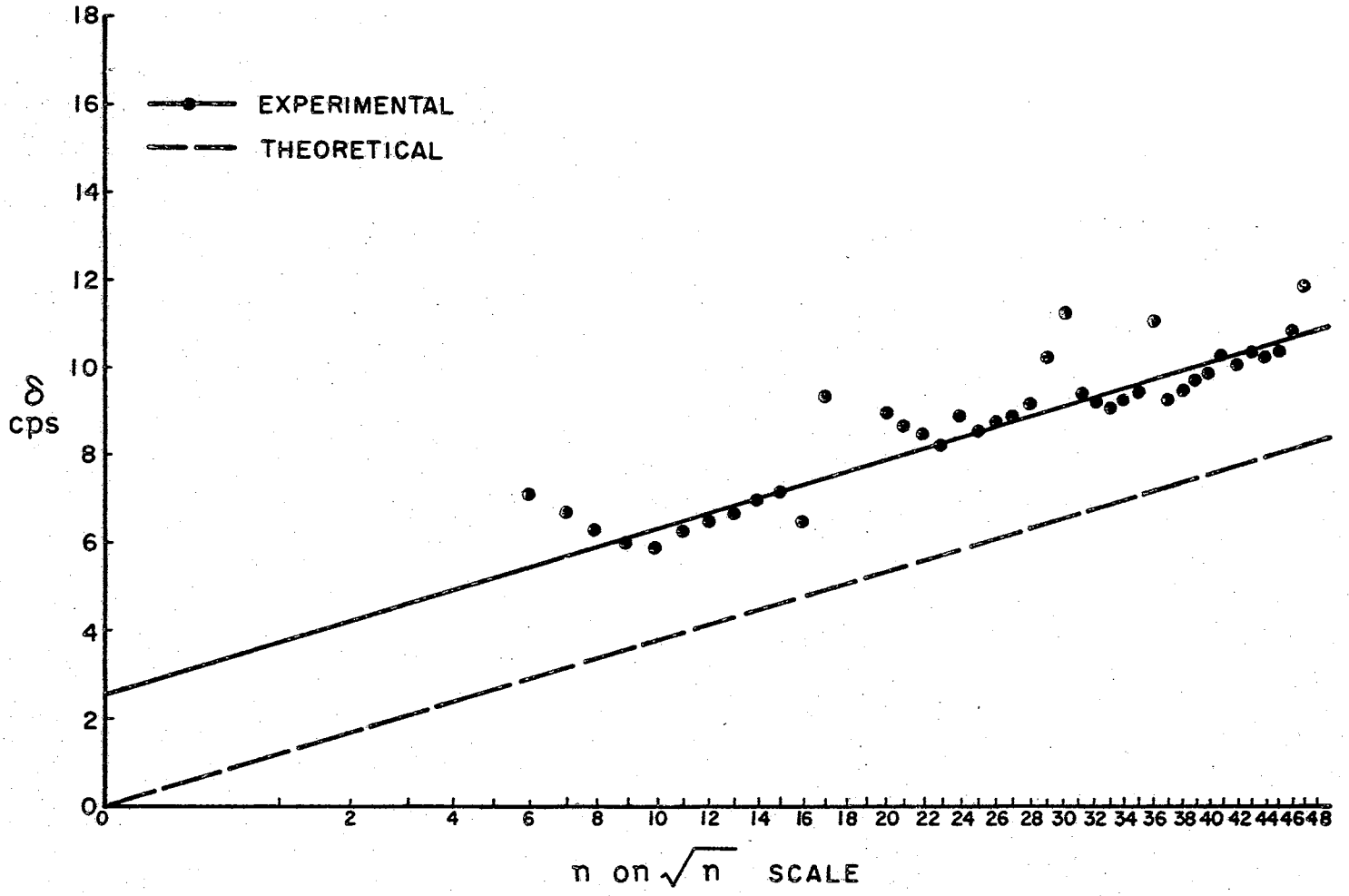

Figure 22. Absorption in nitrogen at 151°C and 5.0 atmospheres absolute, where n is the harmonic number and δ is the width of the resonance peaks, between the half power points

prominent.

The data appearing in Figure 18 serve as a standard to which absorption measurements can be referred when effects of relaxation are present.

In order for the resonance tube to be useful at different temperatures and pressures, it must be calibrated, as above, for each new temperature and pressure combination. Figures 19-22 show absorption in nitrogen at several different pressure-temperature combinations. The quantitative results from these calibration curves are as follows--

Figure 19: 2 atmospheres absolute and $60^{\circ}C$

$$\delta_{exp} = \delta_{th} + 2.4 = 1.42\sqrt{n} + 2.4;$$

Figure 20: 5 atmospheres absolute and $61^{\circ}C$

$$\delta_{exp} = \delta_{th} + 2.5 = 0.91\sqrt{n} + 2.5;$$

Figure 21: 1 atmosphere absolute and $150^{\circ}C$

$$\delta_{exp} = \delta_{th} + 2.3 = 2.62\sqrt{n} + 2.3;$$

Figure 22: 5 atmospheres absolute and $151^{\circ}C$

$$\delta_{exp} = \delta_{th} + 2.5 = 1.18\sqrt{n} + 2.5.$$

A. Velocity Measurements:

Figure 23 is a plot of $\frac{f_n}{n}$, the resonance frequency, as a function of n, the harmonic number. This curve is from data taken to give the absorption curve in Figure 18. Its purpose is to show how constant the velocity remained during the period of data gathering. A constant velocity for a nonrelaxing gas indicates a constant temperature and pressure, since tube corrections for velocity are small.

Figures 24-27 are presented to show the constancy of temperature and pressure during the data taking periods for absorption measurements shown in Figures 19-22 respectively.

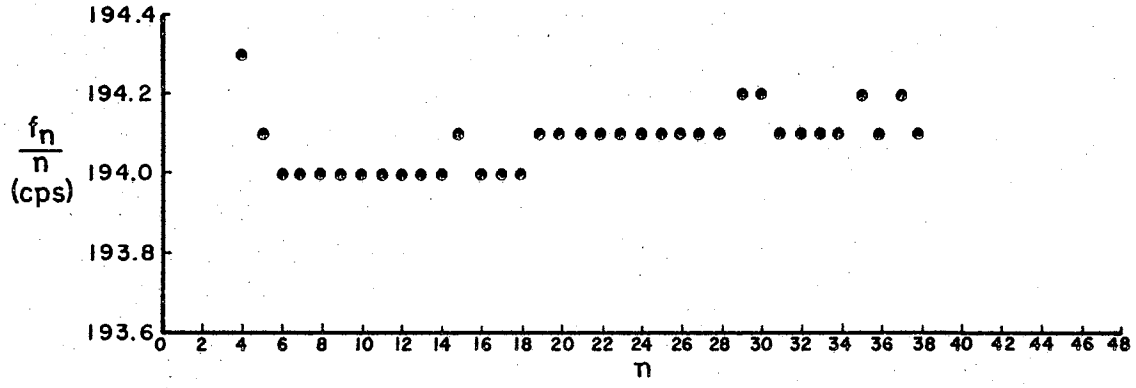

Figure 23. Frequency at resonance, f_n, divided by the harmonic number, n, at 60°C and 1.01 atmosphere absolute versus the harmonic number for nitrogen

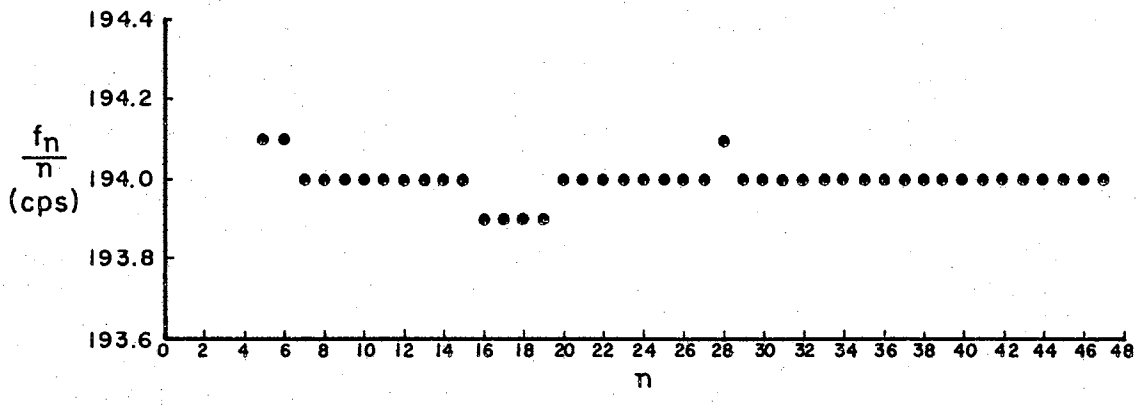

Figure 24. Frequency at resonance, f_n, divided by the harmonic number, n, at 60°C and 2.01 atmospheres absolute versus the harmonic number for nitrogen

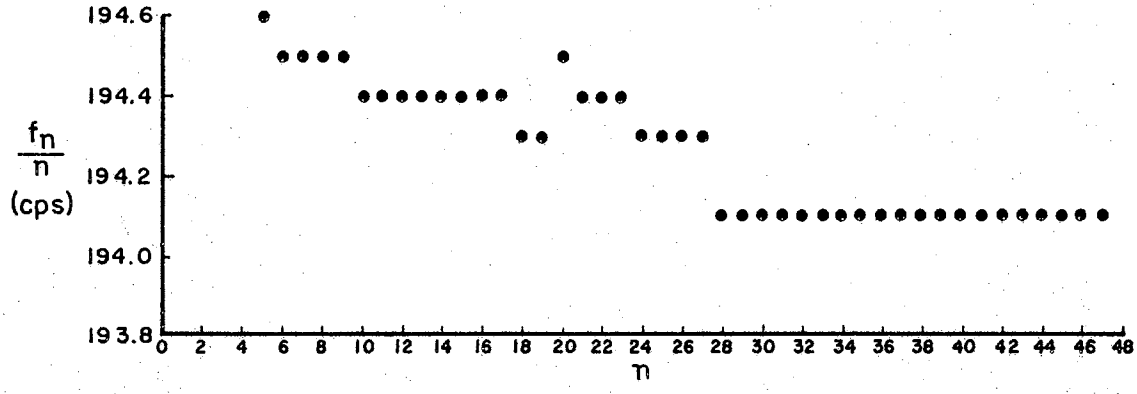

Figure 25. Frequency at resonance, f_n, divided by the harmonic number, n, at 61°C and 5.0 atmospheres absolute versus the harmonic number for nitorgen

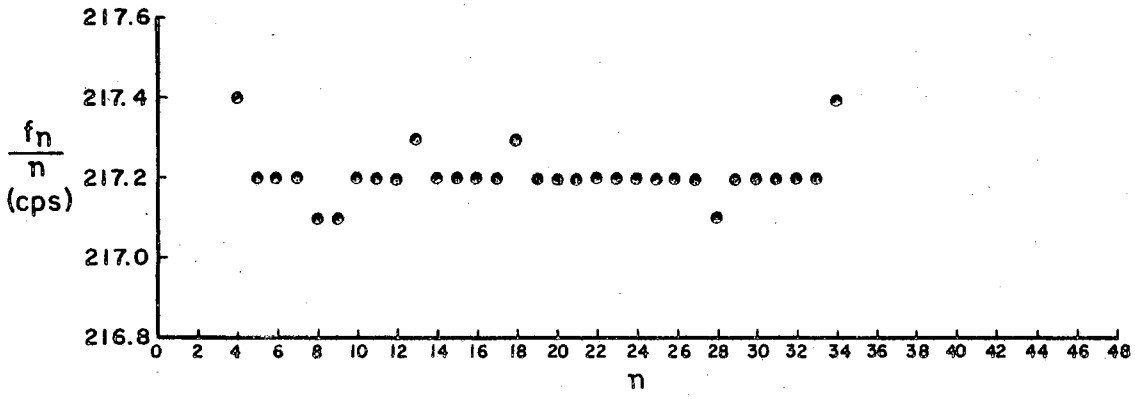

Figure 26. Frequency at resonance, f_n, divided by the harmonic number, n, at 150°C and 1.0 atmosphere absolute versus the harmonic number for nitrogen

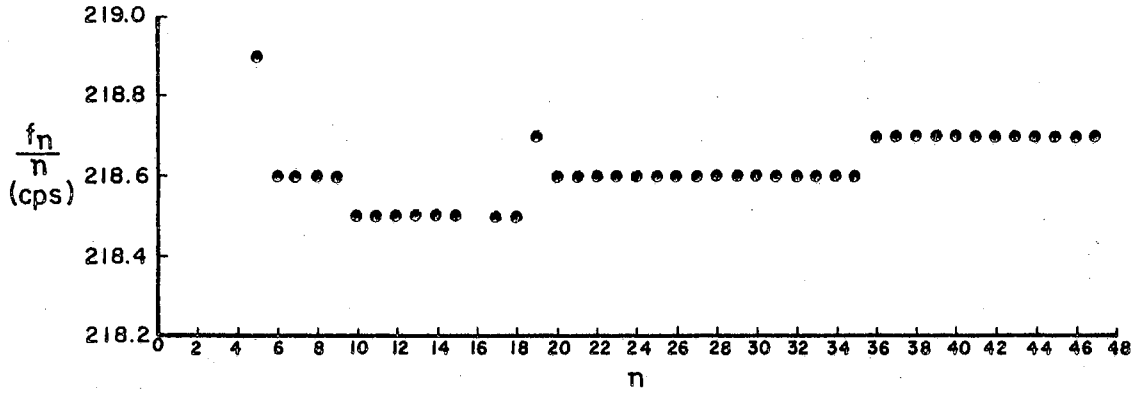

Figure 27. Frequency at resonance, f_n, divided by the harmonic number, n, at 151°C and 5.0 atmospheres absolute versus the harmonic number for nitrogen

CHAPTER V

ERROR ANALYSIS

In Chapter II, the assumption that $\frac{\delta}{f_a} \ll 2\pi$ is made. From Chapter IV, the experimental results justify this assumption as indicated by the following analysis.

Experiment	Minimum δ/f_a	Maximum δ/f_a	$2/\pi$
60°C and 1.01 Atm.	0.038	0.079	.637
60°C and 2.01 Atm.	0.032	0.066	.637
61°C and 5.0 Atm.	0.025	0.047	.637
150°C and 1.0 Atm.	0.041	0.085	.637
151°C and 5.0 Atm.	0.027	0.054	.637

This means that $\frac{\delta}{f_a} \sim \frac{1}{10}\left(\frac{2}{\pi}\right)$ for all the experiments and since $f_a = \frac{c}{2l'}$, by substitution $\frac{\pi l'\delta}{c} \sim \frac{1}{10}$ and by use of Equation (11) $\sigma l' \sim \frac{1}{10}$. Hence, the small angle approximations used in deriving Equation (9) are justified.

In calculating absorption due to boundary effects in Chapter IV, end effects are ignored as well as classical absorption in the bulk of the gas. As pointed out by Parker[1], these effects should be negligible compared to wall absorption. However, the apparatus designed in this thesis apparently absorbs a constant amount of sound energy in addition to that absorbed by

---

[1] J. G. Parker, J. Chem. Phys., 34, 1763 (1961).

the tube walls.

The origin of the extra, constant, absorption is not understood, but possibly is due to the geometry of the ends of the resonance tube. The driver end of the tube has a 1/16 inch opening for evacuating and filling purposes. The other end of the tube has a hole which is not completely filled by the microphone probe tube, an .008 inch gap surrounds the probe. The nitrogen used during the calibration procedure in Chapter IV is "Lab Grade" and is assumed to be pure enough not to cause the extra absorption. If the "unwelded bellows" designed by Hall[2] should leak, radiations from the back of the piston would adversely affect absorption measurements.

Further work with the design of the driver is needed as indicated in Chapter IV. Presently the first few harmonics are distorted by the mechanical resonance of the driver and other unknown causes. Transmitted sound along the tube walls interferes with absorption measurements at frequencies from about 3500 to 3900 cps and about 6000 to 6600 cps. It may prove possible to acoustically insulate the microphone from the resonance tube, thus helping solve the transmitted sound problem.

Even with the design problems outlined in the preceding paragraphs, the apparatus in its present condition should be useful in detecting extra absorption due to relaxation. The theoretical wall absorption could be calculated for the relaxing gas then the constant absorption, found during calibration, could be added. Any extra absorption would be due to relaxation.

The statement in the above paragraph is based upon the reproducibility

---

[2]Heinz Hall, Machine Shop Foreman, Oklahoma State University, Physics Department.

of experimental data as found during the calibration process in Chapter IV. The velocity curves, Figures 23-27, indicate good temperature control and frequency measurements. The following analysis of the 60^{o}C-2.01 atmosphere data further indicates the degree of data reproducibility. In this analysis, the Probable Error in δ, based on three trials, is calculated for several of the resonance peaks (harmonics).

Harmonic, n	δ Trial #1	δ Trial #2	δ Trial #3	Probable Error
8	6.6 cps	6.7 cps	6.8 cps	±.04 cps
9	6.7 cps	7.0 cps	6.8 cps	±.06 cps
10	7.0 cps	6.9 cps	7.0 cps	±.03 cps
11	7.3 cps	7.1 cps	7.4 cps	±.06 cps
20	9.8 cps	10.1 cps	10.2 cps	±.08 cps
21	9.3 cps	9.5 cps	9.5 cps	±.05 cps
22	9.7 cps	9.6 cps	9.3 cps	±.08 cps
23	9.8 cps	9.9 cps	9.7 cps	±.04 cps
24	10.3 cps	10.5 cps	10.4 cps	±.04 cps
25	10.9 cps	10.3 cps	10.3 cps	±.13 cps
26	10.7 cps	10.5 cps	10.5 cps	±.05 cps
27	10.2 cps	10.4 cps	10.3 cps	±.04 cps
28	10.2 cps	10.3 cps	10.3 cps	±.03 cps
29	11.2 cps	11.2 cps	11.0 cps	±.05 cps
30	10.3 cps	10.4 cps	10.7 cps	±.08 cps

The accuracy of the electronic gear as well as the acoustic apparatus affects the accuracy of the experiment. The two instruments whose errors enter most directly into the absorption measurements are the Hewlett

Packard 5212A counter and the Hewlett Packard 400D vacuum tube voltmeter.

The frequency is counted for 10 sec. for each reading, giving an accuracy of plus or minus 0.1 cycle or since δ is the difference of two readings the accuracy is plus or minus 0.2 cycles. For the experiments in Chapter IV, δ varies from about 5 to 18 cps, thus the counting accuracy varies from about 4% to 1% respectively. The higher the pressure the larger the counting error. This may partly account for the increased spread of data with increased pressure as discussed in Chapter IV. The use of the down-10 db points instead of the down-3 db points improves the counting accuracy by a factor of 3 and should be used for the narrow peaks if noise does not interfere.

It is estimated that the voltmeter can be read with an accuracy of about 4%; thus, the δ measurements in Chapter IV are subject to a possible variation of about 8% to 5% by addition of the possible errors of cycle counting and db reading on the voltmeter. The 8% applies to narrow peaks, on the order of 5 cps wide, and the 5% applies to the wide peaks, on the order of 18 cps wide, thus producing a spread of from about 0.40 cps to about 0.90 cps.

The operator's success in locating the resonance peaks and down-3 db points with the fine adjustment on the oscillator is another possible source of error, but with care, these points can be located with good accuracy.

To summarize this discussion of error analysis, the counting accuracy could be improved by counting for longer periods of time and a more accurate voltmeter would improve the accuracy of measuring the down-3 db points; but, considering the Probable Error calculation made earlier in this chapter, fair data may be taken with the present arrangement.

CHAPTER VI

SUMMARY

An acoustic instrument with which to measure sound absorption and velocity in a gas is designed, constructed and partially calibrated. The Kundt resonance tube technique is followed for the basic design. Modifications are made so that the tube will operate over a wide range of temperatures and pressures. Accessory apparatus designed and constructed include an all stainless steel high pressure gas handling system and an oven in which to heat the resonance tube.

During the calibration procedure, a constant amount of extra sound absorption is discovered and possible origins discussed. The apparatus may now be used to measure relaxation times in oxygen at various temperature-pressure combinations, with proper calibration; but further work with the driver design would significantly improve the usefulness of the device.

The author has gained an inestimable amount of research knowledge while attempting to solve this design, construction and calibration problem. His future teaching should be enhanced by his many experiences while undertaking this work. The trial and error approach which had to be used in developing part of the apparatus will certainly make the teacher more cognizant of the necessity for being considerate of attempts made by students as they use the scientific method in their development.

BIBLIOGRAPHY

1. Beranek, L. L., Acoustics, McGraw-Hill Book Co., Inc., N. Y., Toronto and London, 1954.

2. Blackman, V. H., J. Fluid Mech., 1, 61, (1956).

3. Clark, A. V. and M. C. Henderson, J. Acoust. Soc. Am., 35, 1909 (1963).

4. Cottrell, T. L. and J. C. McCoubrey, Molecular Energy Transfer in Gases, Butterworths, London, 1961.

5. Gaydon, A. G., and I. R. Hurle, The Shock Tube in High Temperature Chemical Physics, Reinhold Publishing Corp., N. Y., 1963.

6. Henderson, M. C., J. Acoust. Soc. Am., 32, 1511 (1960).

7. Henderson, M. C., J. Acoust. Soc. Am. 34, 349 (1962).

8. Henderson, M. C. and G. J. Donnelly, J. Acoust. Soc. Am. 34, 779 (1962).

9. Herzfeld, K. F., Thermodynamics and the Physics of Matter, Princeton University Press, Princeton, New Jersey, 1955, Vol. 1, Sec. H.

10. Herzfeld, K. F. and T. A. Lotovitz, Absorption and Dispersion of Ultrasonic Waves, Academic Press, Inc., New York, 1959.

11. Herzfeld, K. F. and F. O. Rice, Phys. Rev., 31, 691, (1928).

12. Holmes, R., F. A. Smith and W. Tempest, Proc. Phys. Soc., 81, 311 (1963).

13. Hueter, Theodor F. and Richard H. Bolt, Sonics, John Wiley & Sons, Inc., New York, Chapman and Hall, Limited, London, 1955.

14. Hunter, J. L., Acoustics, Prentice-Hall, Inc., N. J., 1957.

15. Kinsler, Lawrence E. and Austin R. Frey, Fundamentals of Acoustics, 2nd Ed. John Wiley & Sons, Inc., New York and London, 1963.

16. Knötzel, H. and L. Knötzel, Ann. Phys. Lpz., 2, 393, (1948).

17. Landau, L. and E. Teller, "Physik Z. Sowjetunion" 10, 34 (1938).

18. Morse, Phillip M., Vibration and Sound, Mc-Graw-Hill Book Co., Inc., New York and London, 1936.

19. Oberst, H., Akust. Z. 2, 76 (1937).

20. Parker, J. G., J. Chem. Phys., 34, 1763 (1961).

21. Randall, Robert H., An Introduction to Acoustics, Addison-Wesley Press, Inc., Cambridge 42, Mass., 1951.

22. Rayleigh, Lord, Theory of Sound, Dover Publications, New York, 1945.

23. Roberts, Richard W., "An Outline of Vacuum Technology" General Electric Report No. 64-RL-3394C (Revised) September, 1964.

24. Schnaus, U. E., J. Acoust. Soc. of Am. 37, 1 (1965).

25. Shields, F. D., J. Acoust. Soc. Am. 34, 271 (1962); 32, 180 (1960); 31, 248 (1959); 29, 450 (1959); 29, 410 (1957).

26. Shields, F. Douglas and Robert T. Lagemann, J. Acoust. Soc. of Am. 29, 470 (1957).

27. Shields, F. D. and Kun Pal Lee, J. Acoust. Soc. of Am. 35, 251 (1963).

28. Smith, D. H. and H. J. Wintle, J. Fluid Mech., 9, 29 (1960).

29. Smith, F. A. and W. Tempest, J. Acoust. Soc. Am., 33, 1626 (1961).

30. "Steel Products Manual", American Iron and Steel Institute, New York 17, N. Y., April, 1963.

31. Wood, A. B., A Textbook of Sound, The MacMillan Co., N. Y., 1955.

APPENDIX A

PROPERTIES OF STAINLESS STEEL TYPE 304

Sizes, in	Form and Treatment	Tensile Strength, psi	Yield Strength (offset: 0.2 per cent), psi	Elongation in 2 in., per cent	Reduction of area per cent	Impact resistance, ft.-lb. Izod	Hardness Number: Brinell (3000-kg. load 10-mm. ball)	Hardness Number: Rockwell	Endurance limit (fatigue), psi	Cold bend. deg.
	Sheet: Annealed	84,000	42,000	55				B-80	35,000	180
	Strip: Annealed	84,000	42,000	55				B-80	35,000	180
	Plate: Annealed	82,000	35,000	60	70	110	149		35,000	180
All	Bars: Annealed	85,000	35,000	60	70	110	149		34,000	
1	Ann.&Cold Drawn	100,000	60,000	45			212			
7/8	Cold Drawn High Tensile	125,000	95,000	25			277			
1½	Cold Drawn High Tensile	110,000	75,000	60		90	240			

Type 304 is a low carbon austenitic chromium nickel stainless and heat resisting steel somewhat superior to Type 302 in corrosion resistance.

Type 304 is nonmagnetic when annealed, but is slightly magnetic when cold worked.

Chemical Composition, Per Cent

C	Mn	P	S	Si	Cr	Ni
0.08 Max.	2.00 Max.	0.045 Max.	0.030 Max.	1.00 Max.	18.00 20.00	8.00 12.00

Physical Properties in the Annealed Condition

Modulus of elasticity in tension, psi	28.0×10^6
Modulus of elasticity in torsion, psi	12.5×10^6
Density, lb. per cu. in.	0.29
Specific electric resistance at room temperature, microhm-centimeters	72
Specific heat, Btu. per lb. per deg. Fahr. (32 to 212 F.)	0.12
Thermal conductivity, Btu. per hr. per sq. ft. per ft. per deg. Fahr.	
212 F.	9.4
932 F.	12.4

Mean coefficient of thermal expansion per deg. Fahr.	
32 to 212 F.	9.6×10^{-6}
32 to 600 F.	9.9×10^{-6}
32 to 1000 F.	10.2×10^{-6}
32 to 1200 F.	10.4×10^{-6}
Melting point range, deg. Fahr.	
2550 to 2650	

Thermal Treatment

Initial forging, deg. Fahr.	2100 to 2300
Annealing, deg. Fahr. Cool rapidly from	1850 to 2050
Hardening, deg. Fahr. Hardenable by cold work only	

APPENDIX B

DERIVATION OF EVACUATION TIME EQUATION[1]

Three classes of gas transport or flow are turbulent flow, viscous flow, and molecular flow. A calculation need only be concerned with viscous flow and molecular flow when dealing with vacuum systems.

The ratio of mean free path, λ, to a characteristic dimension of the system, a, is called the Knudsen number and is used to characterize the type of gas flow. For example

if $\frac{\lambda}{a} < 0.01$, viscous flow exists;

if $\frac{\lambda}{a} < 1.00$, molecular flow esists; and

if $0.01 < \frac{\lambda}{a} < 1.00$, an intermediate kind of flow exists.

The mean free path of air at $25^{\circ}C$ is about equal to

$$\lambda_{(\text{air } 25^{\circ}C)} = \frac{5 \times 10^{-3}}{P(\text{torr})} = \text{—— cm.} \qquad (1)$$

Therefore, if $P = 10^{-3}$ torr, the mean free path is 5 cm. or 2 inches; and if $P = 10^{-6}$ torr, λ = 5000 cm or 2000 inches. Thus, for high vacuum systems high Knudsen numbers exist and molecular flow should be considered.

The conductance of a Short Circular Tube for air at $20^{\circ}C$ is given by (molecular flow)

$$C = 12.1 \frac{d^3}{l'} \alpha \frac{\text{liters}}{\text{sec}} \qquad (2)$$

where d is the diameter in cm. of the tube, l' the length in cm. and α depends on $\frac{l'}{d}$. (See Table II)

---

[1] General Electric Report, No. 64-RL-3394C(Revised) Sept. 1964, pp. 19-29, "An Outline of Vacuum Technology" by Richard W. Roberts.

The effective speed of the pump at the system, S_{eff}, is given by

$$\frac{1}{S_{eff}} = \frac{1}{S} + \frac{1}{C} \tag{3}$$

where S is the speed of the pump at its inlet and C is the conductance of the connecting tube. Solving for S_{eff} gives

$$S_{eff} = \frac{SC}{S + C} \tag{4}$$

If a very fast pump is used, i.e., $S > C$, then $S_{eff} = C$, or, the effective pumping speed can never exceed the conductance.

Pump down time:

The time to pump a system of volume V from P_1 to P_2 with a pump of speed S may be estimated by using the expression

$$t = 2.3 \frac{V}{S} \log \frac{P_1}{P_2} \text{ sec}, \tag{5}$$

where V is in liters and S in liter/sec.

TABLE II

VALUES OF α FOR SHORT TUBE CALCULATIONS

$\frac{l'}{d}$	α
0.05	0.036
.08	.055
.1	.068
.2	.13
.4	.21
.6	.28
.8	.30
1.0	.38
2	.54
4	.70
6	.77
8	.81
10	.84
20	.91
40	.95
60	.97
80	.98
100	1.00

VITA

Denver L. Prince

Candidate for the Degree of

Doctor of Education

Thesis: THE DESIGN AND CONSTRUCTION OF AN ACOUSTIC INSTRUMENT TO INVESTIGATE THE VIBRATIONAL RELAXATION TIMES IN OXYGEN AT HIGH TEMPERATURES

Major Field: Higher Education in Physics

Biographical:

Personal Data: Born at Beaton, Arkansas, October 16, 1932, the son of Olis M. and Kathleen Prince.

Education: Attended grade schools in Arkansas and California; graduated from Magnet Cove High School, Route 5, Malvern, Arkansas, in 1950; received the Bachelor of Science degree from Henderson State Teachers College, Arkadelphia, Arkansas, with a major in Chemistry, in May 1954; received the Master of Science-Education degree from the University of Utah, Salt Lake City, Utah, with a major in Science Education, in June, 1958; completed requirements for the Doctor of Education degree in August, 1965.

Professional Experience: Has taught High School Science for four years; one year, 1954-55, at Luxora High School, Luxora, Arkansas, and three years during the period 1955-59 at Magnet Cove High School, Route 5, Malvern, Arkansas. Was appointed as Assistant Professor of Physical Science at the Arkansas State Teachers College, Conway, Arkansas, in September, 1959, and has taught Chemistry and Physics there for four years. Has been a research assistant in Physics at the Oklahoma State University during 1964-65. Starts new appointment as Head of Physics Department at the Arkansas State Teachers College in July, 1965.